Increased sexual dimorphism evolves in a fossil stickleback following ecological release from fish piscivores

Matthew Stuart[1,2], Allison Ozark[3], Raheyma Siddiqui[3], Akhil Ghosh[1,2]
Samantha Swank[3], Michael A. Bell[4], Gregory J. Matthews[1,2], and Yoel E. Stuart[3,+]

[1] Department of Mathematics and Statistics, Loyola University Chicago, Chicago, IL, U
[2] Center for Data Science and Consulting, Loyola University Chicago, Chicago, IL, U
[3] Department of Biology, Loyola University Chicago, Chicago, IL, USA
[4] University of California Museum of Paleontology, Berkeley, CA, USA
[+] Corresponding: ystuart@luc.edu

Abstract

Everyone loves the stickle

Keywords: Stickle

1 Introduction

Ecological release theory suggests that a population's niche should change when important species interactions like resource competition or predation are relaxed or removed (reviewed in Herrmann, Stroud, and Losos (2021)). Removal is posited to create ecological opportunity—i.e., aspects of the niche become newly accessible, and the focal population shifts and/or expands its resource use new resources (Parent and Crespi (2009); Herrmann, Stroud, and Losos (2021)). Ecological release may then be followed by adaptive morphological evolution as traits change to reflect the new niche (Parent and Crespi (2009); Herrmann, Stroud, and Losos (2021)).

For example, a population undergoing ecological release can experience disruptive selection on males and females stemming from intraspecific competition over newly accessible resources (Bolnick and Doebeli (2003); Bolnick and Lau (2008); Cooper, Gilman, and Boughman (2011)). This is predicted to result in intersexual divergence in habitat use and associated phenotypes (Schoener (1968); Shine (1989); Bolnick and Doebeli (2003); Butler and Losos (2007); Bolnick and Lau (2008); Cooper, Gilman, and Boughman (2011); but see Stuart et al. (2021); Blain (2022)). Such competition-driven "intraspecific character displacement" between the sexes is therefore one explanation for the evolution of sexual dimorphism (Pfennig and Pfennig (2012); De Lisle and Rowe (2015); De Lisle and Rowe (2017), De Lisle, Paiva, and Rowe (2018)).

Much of the theory and empirical data for character displacement between the sexes is based on release from resource competition specifically (e.g., Bolnick and Doebeli (2003); Cooper, Gilman, and Boughman (2011); Pfennig and Pfennig (2012); De Lisle and Rowe (2015); De Lisle, Paiva, and Rowe (2018)). However, release from predation might also drive the evolution of increased sexual dimorphism because an absence of predators should generate ecological opportunity (Reimchen and Nosil (2004); Parent and Crespi (2009); Herrmann, Stroud, and Losos (2021)).

Here, we tested the prediction that a release from predation results in the evolution of increased sexual dimorphism using a well-preserved, finely-resolved sequence of a fossil threespine stickleback fish (Gasterosteus doryssus). The sequence in this depositional environment is comprised of two lineages (Bell (2009); Cerasoni, Bell, and Stuart (2024)). Lineage I was a low-armor form with zero to one dorsal spines and highly reduced pelvises, on average. Lineage I lasted for at least 93,000 years before it was replaced by a second lineage, suddenly, likely on the order of years (Bell, Baumgartner, and Oslon (1985); Stuart et al. unpublished data). Lineage II appeared in the depositional environment fully armored, with complete pelvic girdles, two pelvic spines, and three dorsal spines (Bell, Travis, and Blouw (2006); Stuart, Travis, and Bell (2020)). It then immediately began evolving adaptive reduction in its armor traits (Hunt, Bell, and Travis (2008); Stuart, Travis, and Bell (2020)) until it

reached the same low-armor state previously held by lineage I.

The observation of 93,000 years of low-armor stasis in lineage I (Bell, Baumgartner, and Oslon (1985)) and the observation of rapid evolution of armor loss by lineage II, both suggest that this depositional environment lacked piscivorous fish like trout and other salmonids known to prey on modern threespine stickleback. Armor presence in extant threespine stickleback (Gasterosteus aculeatus) correlates strongly with the presence of vertebrate piscivores; populations with less predation pressure typically have less armor (Reimchen (1994), Reimchen and Nosil (2004); Bell et al. (1993); Roesti et al. (2023)). In our paleolake basin, only three fossil trout have been found in the same section of rock that has revealed >20,000 threespine stickleback fossils as well as occasional killifish (Fundulus nevadensis) (Bell (2009); Cerasoni, Bell, and Stuart (2024)). Thus, we reconstruct an evolutionar history in which it is likely that lineage II migrated from a nearby paleolake basin that had predators since it was armored when it arrived (Bell (2009); Cerasoni, Bell, and Stuart (2024)). Lineage II then experienced release from predators in the focal paleolake basin, generating the initial conditions of evolutionary models predicting the evolution of increased sexual dimorphism following ecological release. We test this prediction here.

A major challenge in the study of fossilized sexual dimorphism is assigning sex to individual specimens in the first place (Hone and Mallon (2017); Mallon (2017); Saitta et al. (2020)). This typically cannot be done directly, except for taxa whose sexes are distinguished by the presence or absence of sex-specific characters that preserve well. Instead, paleobiologists often resort to statistical detection of sex and sexual dimorphism, including tests for normality and bimodality in trait distributions (e.g., Mallon (2017)), mixture modeling (e.g., Mallon (2017)), divergence in growth curves (e.g., Saitta et al. (2020)), and emphasis on effect size statistics rather than significance testing (e.g., Saitta et al. (2020)). However, dimorphic signal can be masked by noise introduced by factors both biological and artifactual, including extended growth during ontogeny, age-based bias in survivorship, small sample sizes, time averaging, and taphonomic bias (Godfrey, Lyon, and Sutherland (1993); Koscinski and Pietraszewski (2004); Hone and Mallon (2017); reviewed in Mallon (2017); reviewed in Saitta et al. (2020)). Thus, the best approach to sex classification is likely one of total evidence (Saitta et al. (2020)), including comparison to closely-related, extant species of known sex (e.g., Hone and Mallon (2017); Saitta et al. (2020)).

For our study, we inferred sex in G. doryssus fossils by comparing multivariate morphological trait data from lineage II samples to the same multivariate trait set collected from multiple populations in the closely-related, extant Threespine Stickleback species complex (Gasterosteus aculeatus). Crucially, we determined G. aculeatus sex directly via dissection and/or PCR genotyping. This enabled us to use Multiple Imputation by Chained Equations (MICE; Buuren and Groothuis-Oudshoorn (2011)) to build a predictive multiple imputation algorithm (Little and Rubin (2002)) based on the multivariate morphology of G. aculeatus

individuals of known sex. We applied this algorithm to the fossil data to impute individual sex based on morphology, treating fossil sex as a missing variable. With sex assigned to fossil specimens, we fit a modified Ornstein-Uhlenbeck (OU) (Uhlenbeck and Ornstein (1930)) model using a Bayesian framework that accounts for uncertainty in sex classification to test for evolution of sexual dimorphism in each trait over ~16,000 years of lineage II.

2 Data

2.1 Fossil Specimen Data

We used Gasterosteus doryssus data that were previously reported by Stuart, Travis, and Bell (2020), Voje, Bell, and Stuart (2022), and Siddiqui et al. (2024). Briefly, the data were collected from fossil Series K from Quarry D (Cerasoni, Bell, and Stuart (2024)), dug from an open pit diatomite mine at 9.526° N, 119.094° W, near Hazen, Nevada, USA. Series K consisted of 18 samples taken at ~1000-year intervals, and mean sample times span ~16,363 years. Fish from series K were measured for 16 ecomorphological traits related to armor, swimming, and feeding (Table 1). Series K started at the previously documented horizon when lineage I was replaced by lineage II. The tempo and mode of lineage II armor reduction during this sequence suggests adaptive evolution by natural selection (Hunt, Bell, and Travis (2008)), and we focus on the multivariate evolution of sexual dimorphism by this second lineage.

The lineage II fossil data consist of 814 specimens of unknown sex sampled across 18 time periods spaced ~1000 years apart. Figure 1 shows the sample size for each of the 18 samples. There are at least 22 specimens in each sample with a high of 67 specimens in sample 7.

Table 1: Traits and trait descriptions. 'sc' denotes size correction of trait against standard length. Names of bones follow Bowne (1994) unless otherwise noted.

Trait Name	Trait Code	Trait Description
Standard Length	`stl`	Distance from anterior tip of premaxilla to posterior end of last vertebra (hypural plate)
Dorsal Spine	`mds`	Number of dorsal spines from 0 to 3
Dorsal Fin Ray	`mdf`	Number of bones in the dorsal fin posterior to the third dorsal spine (i.e., soft dorsal fin rays)

Trait Name	Trait Code	Trait Description
Anal Fin Ray	`maf`	Number of bones in the anal fin posterior to the anal spine (i.e., soft dorsal fin rays)
Abdominal Vertebra	mav	Number of vertebrae anterior to the first vertebra contacting an anal fin pterygiophore (Aguirre et al. 2014)
Caudal Vertebra	`mcv`	Number of vertebrae posterior to and including the first vertebra contacting an anal fin pterygiophore (Aguirre et al. 2014)
Pterygiophore number	`mpt`	Number of pterygiophores anterior to but excluding the pterygiophore under the third dorsal spine, which is immediately anterior to and contiguous with the dorsal fin
Pelvic Spine length	`lps.sc`	Length from the base of one pelvic spine above its articulation with the pelvic girdle to its distal tip
Ectocoracoid	`ect.sc`	Length between the anterior and posterior tips of the shoulder girdle base (i.e., ectocoracoid)
Pelvic Girdle	`tpg.sc`	Length between the anterior to posterior tips along midline. If vestigial, the sum of longest anterior-posterior axis for the vestiges
Cleithrum length	`cle.sc`	Length from free dorsal tip to ventral tip of the cleithrum on the anterior margin of the shoulder girdle (i.e., cleithrum)
Premaxilla	`pmx.sc`	Length from the anterior tip of the premaxilla to the distal tip of the ascending process of the premaxilla
Dorsal Spine	`Ds#.sc# = 1,2,or 3`	Length from the base of a dorsal spine above the pterygiophore to its distal tip along the anterior edge

Trait Name	Trait Code	Trait Description
Pterygiophore	`lpt.sc`	Distance between the anterior to posterior tips of the pterygiophore immediately preceding the 3rd dorsal spine (when present)

2.2 Extant Specimen data

To span the gamut of stickleback diversity for our predictive imputation model, we sampled modern stickleback from lakes containing generalist stickleback populations (Hendry et al. (2009); Bolnick (2011)) and from lakes containing benthic-limnetic species pairs (Baumgartner, Bell, and Weinberg (1988); Schluter and McPhail (1992)). The generalist specimens used here were collected by YES in 2013 and were previously described in Stuart et al. (2017) (Table S1). These samples were fixed in formalin, then stained for bone with Alizarin Red in 2013. Benthic and limnetic specimens were kindly loaned by D. Schluter and S. Blain at the University of British Columbia. The Schluter lab collected benthic and limnetic individuals from Enos Lake in 1988 and from Emily Lake, Little Quarry Lake, Paxton Lake, and Priest Lake in 2018 (Table S1). The Enos specimens had been fixed whole in formalin and stored in 40% isopropanol. The specimens from the other lakes were initially preserved whole in 95% ethanol in the field before being gradually transferred to water then formalin in the lab and ultimately stored in 40% isopropanol. In 2019, we stained these specimens for bone using Alizarin Red. We next replicated fossil data collection (Table 1) on these extant specimens. Standard length as well as pelvic-spine length on each side were measured with calipers. We used a dissection microscope to count dorsal spines, pelvic spines, dorsal-fin rays, and anal-fin rays. Right and left-side pelvic girdle lengths and ectocoracoid lengths were measured from ventral photographs taken using a Canon EOS Rebel T7 with a Tamron 16-300 mm MACRO lens mounted on a leveled Kaiser RS1 copy stand. Specimens were held in place for ventral photographs using a small tabletop vise with an attached scale bar. Lateral X-rays were used to measure dorsal spine length, number of pterygiophores anterior to the pterygiophore holding the third spine, length of the pterygiophore just anterior to the third spine, cleithrum length, and pre-maxilla ascending branch length. We also counted vertebrae from the X-rays: abdominal vertebrae were counted anterior to the first vertebra with a haemal spine contacting an anal fin pterygiophore. Caudal vertebrae were posterior, including the first vertebra with the haemal spine contacting the anal fin pterygiophore (following Aguirre, Walker, and Gideon (2014)). X-rays were taken with an AXR Hot Shot X-ray Machine (Associated X-ray Corporation) at the Field Museum of Natural History. Specimens were exposed at 35kV and 4mA. Small fish were exposed for 7s, medium fish for

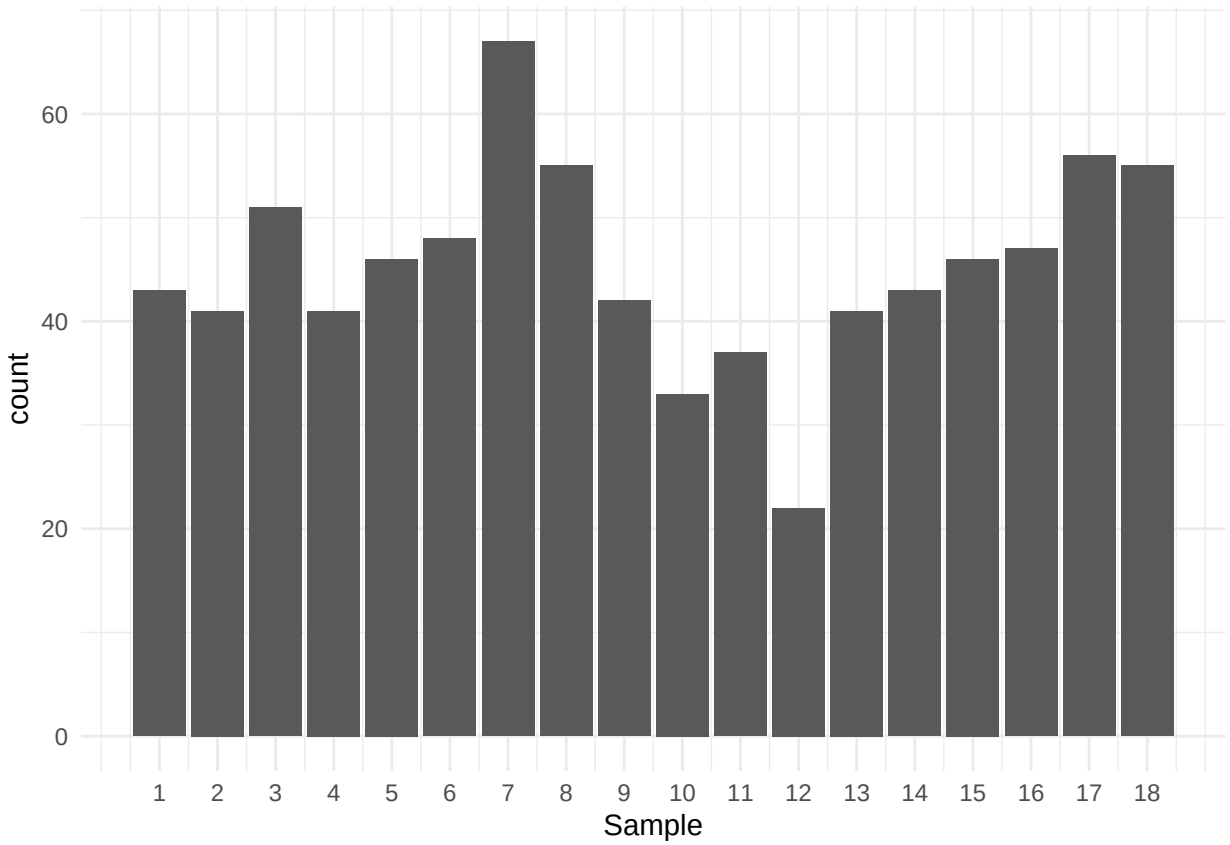

Figure 1: Fossil sample size for each time period

8s, and large fish for 10s. We developed the film and scanned individual images of each fish using the B&W Negatives setting on an Epson Perfection 4990 Photo flatbed at 2400 dpi. Measurements from photographs and X-rays were taken with FIJI (Schindelin et al. (2012)) and its plugin ObjectJ (https://sils.fnwi.uva.nl/bcb/objectj/).

We dissected individuals from the generalist populations (Table S1) to determine sex from the gonads. Individuals from the species-pair lakes (TableS1) were previously sexed by the Schluter lab, using either dissection or a genotyping protocol (Whom, personal communication).

The extant data used here consists of a total of 367 specimens all with known sex (Table S1). Of these, there are 202 and 165 female and male specimens, respectively.

2.3 Outlier analysis and size correction.

To check for outliers, we calculated within-group means and standard deviations for each trait separately for K series fossil specimens (pooled across samples) and for extant specimens (within generalist, benthic, or limnetic categories). We noted trait values greater than 3.0

standard deviations from the mean as potential outliers. We deemed 3.0 s.d. to be a reasonable threshold for detecting errors without excluding biologically relevant values. We checked whether these potential outliers were a result of data entry and collection error and corrected them if they were. We turned the remaining outlier trait values to NAs. We size-corrected continuous traits only, as they varied with size, unlike count traits that are fixed during early development. We regressed each trait on standard length using a mixed-model regression, pooling all specimens, following Stuart et al. (2017). We appended the size corrected data to the uncorrected trait data frame and used all of our data (raw and size-corrected) to build the imputation model described next.

2.4 Missing data imputation, including fossil sex

Briefly, We used multiple imputation (Little and Rubin (2002)) to impute the sex of the fossils. Imputations were performed using the MICE (Buuren and Groothuis-Oudshoorn (2011)) algorithm and implemented in R (Team (2022)) with M = 100 imputations. After imputing the sex, we fit a modified Orenstein-Uhlenbeck (OU; Uhlenbeck and Ornstein (1930)) model to each imputed data set using a Bayesian framework to {THIS NEEDS MORE}. We then quantified sexual dimorphism as the {THIS NEEDS MORE; MAYBE WE CAN WRITE TOGETHER}. We describe the details of the imputation model and OU modeling next.

3 Models

3.1 Imputation Model

Let $\boldsymbol{W}$ be an $(n_{extant} + n_{fossil}) \times 1$ vector of the covariate sex of the stickleback fish and $\boldsymbol{Y}$ be an $(n_{extant} + n_{fossil}) \times K$ matrix of the K phenotypes of interest. Because the sex of the fossilized stickleback fish is unobservable, we further define $\boldsymbol{W} = (\boldsymbol{W}_{extant}^T, \boldsymbol{W}_{fossil}^T)^T$ where $\boldsymbol{W}_{extant}$ and $\boldsymbol{W}_{fossil}$ are the $n_{extant} \times 1$ and $n_{fossil} \times 1$ vectors of the observed extant sex and missing fossil sex, respectively.

AKHIL'S VALIDATION OF THE IMPUTATION MODEL GOES HERE

We impute missing sex for the fossil data by sampling from the posterior predictive distribution $P(\boldsymbol{W}_{fossil}|\boldsymbol{W}_{extant}, \boldsymbol{Y})$ using the multiple imputation by chained equations (MICE) algorithm (Buuren and Groothuis-Oudshoorn (2011)) with predictive mean matching. Traditionally, the choice for the number of completed dats sets is a relatively small number such as $M = 5$ or $M = 10$. However, Zhou and Reiter (2010) recommend a larger number of im-

puted data sets if users intend on performing Bayesian analysis after imputation. Therefore, we imputed $M = 100$ complet datasets.

presumably this also imputes missing data in the other traits? We should probably say that explicitly. -YS

We then pooled all of the draws from the posterior distribution across all the imputed data sets to estimate the posterior distributions of our parameters of interest (i.e., the trait values), rather than usingRubin's combining rules, following Zhou and Reiter (2010). We used these posterior distributions in our Bayesian analysis.

3.2 Bayesian OU modeling

For Bayesian modeling, we dropped the extant data and focused on modeling the evolution of sexual dimorphism through time in the fossils.

DOES THE NEXT SENTENCE CONTRADICT THE PREVIOUS ONE? BELOW, WE SAY THAT WE USED EACH IMPUTED DATA SET. ABOVE, WE SAY THAT WE POOLED ACROSS IMPUTED DATA SETS.-YS For a given imputed dataset, let W_{ij} be the imputed sex and $\boldsymbol{Y}_{ij}$ be the $K \times 1$ vector of phenotypes for stickleback fossil j at time t_i where $i = 1, \ldots, T$ and $j = 1, \ldots, n_t$. Note, we are inputting only the fossil data into our model; connecting to the previous section, W_{ij} and $\boldsymbol{Y}_{ij}$ can be interpreted as $W_{fossil,ij}$ and $\boldsymbol{Y}_{fossil,ij}$. In addition, we denote $Y_{K,ij}$, the last variable in $\boldsymbol{Y}_{ij}$, to be the standard length of the fish,

$$Y_{K,ij} \overset{iid}{\sim} \begin{cases} \mathcal{N}(\mu_{K,ft_i}, \quad \sigma_K^2), & W_{ij} = \text{Female} \\ \mathcal{N}(\mu_{K,mt_i}, \quad \sigma_K^2), & W_{ij} = \text{Male} \end{cases} . \tag{1}$$

It is reasonable to assume that the other continuous traits of stickleback fish will have some correlation with its standard length **(CITATION)**. We account for this by adding an additional parameter, γ_k, into our model. More specifically, if $Y_{k,ij}$ is a continuous trait, then

$$Y_{k,ij} \overset{iid}{\sim} \begin{cases} \mathcal{N}(\mu_{k,ft_i} + \gamma_k Y_{K,ij}, \sigma_k^2), & W_{ij} = \text{Female} \\ \mathcal{N}(\mu_{k,mt_i} + \gamma_k Y_{K,ij}, \sigma_k^2), & W_{ij} = \text{Male} \end{cases} . \tag{2}$$

If $Y_{k,ij}$ is a discrete trait, the conventional method of modelling this data is by fitting a Poisson distribution. However, the Poisson distribution assumes that the mean and variance of $Y_{k,ij}$ are equal ($E(Y_{k,ij}) = \text{Var}(Y_{k,ij})$), while the empirical fossil data may have variances that are smaller than their respective means. To combat this issue, we propose to fit the discrete traits to a generalized Poisson model as defined in (**GeneralizedPoisson?**). Specifically, if

$X \sim GP(\lambda, \alpha)$, then

$$P(X = x) = \begin{cases} \frac{(1-\alpha)\lambda[(1-\alpha)\lambda+\alpha x]^{x-1}\exp\{-((1-\alpha)\lambda+\alpha x)\}}{x!} & (1-\alpha)\lambda + \alpha x \geq 0 \\ 0 & (1-\alpha)\lambda + \alpha x < 0 \end{cases}, \tag{3}$$

where $E(X) = \lambda$ and $Var(X) = \frac{\lambda}{(1-\alpha)^2}$. If $\alpha > 0$, then the variance is greater than the mean, called overdispersion; if $\alpha < 0$, then the variance is greater than the mean, called underdispersion; if $\alpha = 0$, then the model degenerates to a Poisson distribution.

We will use the generalized Poisson to model all of the discrete traits in our dataset. In addition, we assume that the discrete traits abdominal vertebrae (mav) and caudal vertebrae (mcv) also have correlation with the standard length of the fish (**CITATION**). If $Y_{k,ij}$ is one of the above traits, then

$$Y_{k,ij} \sim \begin{cases} GP(\exp\{\mu_{k,ft_i} + \gamma_k Y_{K,ij}\}, \alpha_k), & W_{ij} = \text{Female} \\ GP(\exp\{\mu_{k,mt_i} + \gamma_k Y_{K,ij}\}, \alpha_k), & W_{ij} = \text{Male} \end{cases}. \tag{4}$$

For the other discrete traits, we also assume the above model except we set $\gamma_k = 0$ because of the assumption of no correlation between the standard length and these traits. More specifically, we assume

$$Y_{k,ij} \sim \begin{cases} GP(\exp\{\mu_{k,ft_i}\}, \alpha_k), & W_{ij} = \text{Female} \\ GP(\exp\{\mu_{k,mt_i}\}, \alpha_k), & W_{ij} = \text{Male} \end{cases}. \tag{5}$$

In the above model descriptions, μ_{k,ft_i} and μ_{k,mt_i} model the time-t_i specific mean of phenotype k for female and male stickleback fish, respectively. We point out that, for the discrete traits, the means are represented by $\exp\{\mu_{k,ft_i}\}$ and $\exp\{\mu_{k,mt_i}\}$ for ease of use in our modeling technique. We further set

$$\mu_{k,gt_i} = \beta_{0,kg} + \beta_{1,kg} t_i + u_{k,gt_i}, \tag{6}$$

for $g \in \{f, m\}$ where $\beta_{0,kg}$ and $\beta_{1,kg}$ are regression parameters of phenotype Y_k for each sex, accounting for the possibility of a time-dependent trend in the mean structure, and u_{k,gt_i} is the corresponding residual. To account for potential correlations between the residuals for a given trait k and sex g, we fit an Ornstein-Uhlenback (OU) process (Uhlenbeck and Ornstein (1930)). More specifically, define $du_{k,gt} = u_{k,g(t+dt)} - u_{k,gt}$, the change in u_k, gt for a given trait k and sex g over a miniscule time period dt. The OU process is defined as

$$du_{k,gt} = -\kappa_k u_{k,gt} dt + \tau_k dW_t, \tag{7}$$

where κ_k is a parameter associated with the correlation between $u_{k,gt}$ and $u_{k,g(t+dt)}$, τ_k is the

standard deviation of the OU process, and W_t is a standard Brownian motion. As shown in Uhlenbeck and Ornstein (1930), the closed form solution for the SDE in (7) is

$$u_{k,gt_i} \overset{iid}{\sim} \mathcal{N}\left(u_{k,gt_{i-1}} \exp\{-\kappa_k(t_i - t_{i-1})\}, \frac{\tau_k^2(1 - \exp\{-2\kappa_k(t_i - t_{i-1}))\}}{2\kappa_k}\right) \tag{8}$$

for $i = 2, \cdots, T$. In a traditional OU process, the initial value u_{k,gt_1} is assumed to be a (potentially unknown) constant, and we discuss the procedure for estimating this value below.

In our empirical study, we analyze the following four nested models for the mean process outlined in (6):

- OU with Trend: The mean process for each phenotype $k = 1, \cdots, K$ and $g \in \{f, m\}$ as previously defined.
- OU with No Trend: No linear trend on the mean processes and the overall mean of the phenotype is constant for each sex. This is achieved by setting $\beta_{1,kg} = 0$ in (6) for $k = 1, \cdots, K$ and $g \in \{f, m\}$
- No OU with Trend: No random fluctuations on the mean processes, i.e. the OU process assumption is not needed. This is achieved by setting $u_{k,gt_i} = 0$ in (6) for $k = 1, \cdots, K$, $g \in \{f, m\}$, and $i = 1, \cdots, T$.
- No OU with No Trend: The mean for a specific trait and specific sex at each time point is a constant value. This is achieved by setting $\beta_{1,kg} = 0$ and $u_{k,gt_i} = 0$ in (6) for $k = 1, \cdots, K$, $g \in \{f, m\}$, and $i = 1, \cdots, T$.

Because we are fitting a dataset with a stochastic structure on phenotype means, and we are interested in the distribution of the overall structure of these means, we analyze the data via a Bayesian analysis <THIS LAST CLAUSE DOESN'T FOLLOW FROM THE BECAUSE CLAUSE. BETTER EXPLAIN WHY BAYES IS GOOD HERE>. Bayesian data analysis is also more naturally used when we have to impute data (**CITATION**). To aid in the sampling procedure for the discrete phenotypes, we declare

Priors: To aid in the sampling procedure for the discrete phenotypes, we declare $\phi_k = \log\left(\frac{\alpha_k - \max_{i,j}(-\lambda_{k,ij}/y_{k,ij})}{1-\alpha_k}\right)$ where $\lambda_{k,ij} = \begin{cases} \exp(\mu_{k,ft_i} + \gamma_k Y_{K,ij}) & W_{ij} = \text{Female} \\ \exp(\mu_{k,mt_i} + \gamma_k Y_{K,ij}) & W_{ij} = \text{Male} \end{cases}$. This transformation is performed to ensure our algorithm can properly sample from the posterior distribution of interest.

For $k = 1, \cdots, K$,

$$
\begin{aligned}
u_{k,gt_1} &\overset{iid}{\sim} \mathcal{N}(0, \tau_{0,k}) \\
\sigma_k &\overset{iid}{\sim} \mathcal{N}(0, 10) I_{\{\sigma > 0\}} \\
\sigma_k &\overset{iid}{\sim} \mathcal{N}(0, 10) \\
\tau_k &\overset{iid}{\sim} \mathcal{N}(0, 10) I_{\{\tau > 0\}} \\
\tau_{0,k} &\overset{iid}{\sim} \mathcal{N}(0, 20) I_{\{\tau > 0\}} \\
\kappa_k &\overset{iid}{\sim} \mathcal{N}(0, 1) I_{\{\kappa_g > 0\}} \\
\gamma_k &\overset{iid}{\sim} \mathcal{N}(0, 5) \\
\beta_{0,kg} &\overset{iid}{\sim} \mathcal{N}(0, 100) \\
\beta_{1,kg} &\overset{iid}{\sim} \mathcal{N}(0, 3)
\end{aligned}
\tag{9}
$$

We also note that, for the discrete phenotypes in equations (4) and (5), there is no σ_k, and is not sampled, and for the continuous phenotypes in equation (2), there is no ϕ_k and is not sampled.

All models were built using Team (2022) and (**S**TAN)

Cornuault (2022) Bayesian OU model.

4 Results

<WE NEED RESULTS SECTION DESCRIBING THE RESULTS OF AKHIL'S MULTIPLE IMPUTATION, BOTH THE TESTS OF HOW WELL THE MODEL WORKED CLASSIFYING MODEL SAMPLES, AND SUMMARY STATISTICS OF FOSSIL IMPUTATION RESULTS -YS>

Within each trait, the model with the lowest DIC was chosen for that trait . All subsequent results presented here use the model with the lowest DIC individually by trait .

Table 4.1 reports the results of model fitting. X of the Y traits were best fit by a trend model. Best models included an OU component for caudal and abdominal vertebra number (mcv, mav), pelvic spine length (lpt) and standard length (stl). Caudal vertebra number was the only trait best fit by a model including both a trend and an OU component. This implies that not only does caudal vertebra size have a linear trend across sex <WHAT DO YOU MEAN BY LINEAR TREND ACROSS SEX?>, but the average size at one time period is highly correlated with the average size at the next time period <I'VE ALWAYS FOUND

THAT THIS AID TO MODEL INTEPRETATION IS BETTER IN THE METHODS, JUST AFTER THE MODELS ARE DESCRIBED>.

Yoel's interpretation of the above paragraph. Taking the model with the lowest DIC score as the best model for each trait, we found that cle, ds1, lps, and pmx did not fit either the trend model or the OU model for male-female trait mean differences. In contrast, we found a trend through time in male-female trait mean differences (i.e., sexual dimorphism) for mcv, ds2, ds3, ect, maf, and mdf. This suggests that these traits changed their dimorphism from one time period to the next, with an overall tendency toward ???GREATER/LESS??? dimorphism. IS THIS CORRECT? - YS We found evidence for an OU process but no trend for lpt, mav, and stl, suggesting that these traits varied through time, about a fixed value for dimorphism. Finally, we found evidence that change in mcv fitted both a trend an an OU process, meaning ??? WHAT BIOLOGICALLY ???.

HOW DO WE RECONCILE THE PRESENCE OF TRENDS IN THESE MODELS WITH AN ABSENCE OF VISIBLE TRENDS IN FIGURES 2 THROUGH 4? I WONDER IF THIS RESULT PARAGRAPH BELONGS BEST AT THE END OF THE RESULTS, RATHER THAN THE BEGINNING. CONSIDER THE STATISTICAL EVIDENCE FOR TRENDS AND OU AFTER WE'VE WALKED THE READERS THROUGH VISUAL EVIDENCE FOR CHANGE.

4.1 Best fitting models

	OU	No OU
Trend	mcv	ds2, ds3, ect, maf, mdf
No Trend	lpt, mav, stl	cle, ds1, lps, pmx

4.2 Sexual Dimorphism

Table **??** shows the posterior probability of the differences in the means between male and female specimens at each time point. Probabilities near 0.5 indicate very little difference in the means whereas probabilities far from 0.5 indicate sexual dimorphism with values of 0 and 1 indicating larger mean values for females and males, respectively. These results are shown graphically in figure 3.

Figure 2 shows the posterior mean difference for males versus females (values above 0 indicate means that were greater for males versus females). The full posterior distributions over time for all traits are shown in the appendix.

Traits such as standard length (stl), anal fin ray (maf), dorsal fin ray (mdf), premaxilla (pmx), and dorsal spine 1 (ds1) demonstrate constant sexual dimorphism with all but the last having learger mean values in male sepcimen. Other traits such as abdominal vertebra (mav), caudal vertebra (mcv), and pelvic spine length (lps) don't appear to have any discernable sexual dimorphism in the means. Dorsal spine 3 (ds3) exhibits sexual dimorphism that changes over time. The mean number of dorsal spine 3 begins larger for females for the earliest observed time periods. Over time, however, this switches and the male specimens exhibit larger mean values for the latest observed time periods.

Yoel's interpretation of the three paragraphs above. Male and female G. doryssus differ for some traits, indicating detectable sexual dimorphism. This is evidenced by traits with substantial differences in male and female posterior means (i.e., deviation from 0 in Figure 2), supported by posterior probabilities that deviate from 0.5 (Figure 3). For example, males are larger than females by 3-8mm on average through time (stl panel in Figure 2), with a posterior probability for that mean difference above 70 percent through time (Figure 3). In contrast, the number of abdominal vertebrae (mav) fluctuates about 0 (Figure 2), with posterior probabilities fluctuating about 50 percent through time (Figure 3). Table **??** in the Supplementary Material summarizes the posterior probabilities that male means differ from female means by trait and sample.

can we move mu-diff-plot and prob0-plot here?

4.3 Changes over time

Table **??** shows the probability that the posterior distribution of the differences in the mean is greater than the posterior distribution of the differences at the first time point. Values near 0.5 indicate very little difference between the distributions whereas values closer to 0 and 1 indicate changes in the distributions with values of 1 meaning the difference in means has shifted towards males having a larger mean and values of 0 indicating the difference in means has shifted towards larger means in females. These results are shown graphically in figure 4.

The amount of sexual dimporphism over time does not change substantially for a majority of the trait observed here (i.e. cle, ds1, ds2, ect, lps, lpt, mav, mcv, pmx, stl). Traits that trend away from the mean difference at the first observed time point include dorsal spine 3 (ds3), anal fin ray (maf), and dorsal fin ray (mdf).

The posterior mean of the mean number of dorsal spine rays at the first observed time point is 2.29 for males and for females it is 2.45. At the last observed time point, the average number for males and female both dropped to 1.265 and 1.185 for males and females, respectively. This resulted in a mean number of dorsal spine 3 lost by males of 1.027 and for females it

was 1.264. This resulted in a change of the mean difference from time point 1 to time point 18 of 0.236. Basically, males and females both lowered the mean number of dorsal spine 3, but females lowered their mean more than the males.

We also observed a change in the differences between males and females for the number of bones int he anal fin ray (maf) and the number of bones in the dorsal fin ray. The difference in the means of males versus females for anal fin ray bones changed by 0.152 over the course of the observed time periods. This change was driven mostly by the change in females. At the first observed time period the had on average 8.291 bones dropping to 8.170 over the 18 times periods observed. Whereas for males the change in means rose only from 8.518 to 8.549, about 0.0316 bones on average.

A similar change in the difference of the means over time was observed for the number of bones in the dorsal fin (mdf). However, unlike maf, this change in sexual dimporhism was driven entirely by the males. The mean change for females over the 18 observed time periods was only 0.0055 with the average number of dorsal fin bones for females starting at 9.287 and the final observed mean of 9.281 resulting in almost no change in the mean. For males, the average number of dorsal fin bones at the first time point was about 9.568 dropping to 9.734 over the course of the observed time periods for a gain of 0.166 bones on average.

Yoel's interpretation of the five paragraphs above. Figure 4 shows the posterior probability that the mean male-female difference at time t is different from the male-female difference at time zero. In other words, Figure 4 plots whether the sexual dimorphism changes in subsequent samples, always relative to the first sample. The amount of sexual dimporphism over time does not change substantially for a majority of the traits (i.e. cle, ds1, ds2, ect, lps, lpt, mav, mcv, pmx, stl; Figure 4). Traits that change in dimorphism are anal fin ray (maf), and dorsal fin ray (mdf), and dorsal spine 3 (ds3).

For example, females at time zero averaged 8.29 rays in the anal fin, dropping to 8.17 rays in the final sample. Males averaged 8.52 anal fin rays in the first sample and 8.55 in the last sample. Thus, the difference between males and females started at 0.23 and ended at 0.38, an increase in sexual dimorphism. In contrast, the sign on dimorphism flipped for ds3. The posterior mean length of the third dorsal spine is 2.29mm for males and 2.45mm for females. By the end of the sequence, mean ds3 for males was 1.27 for males and 1.19 for females. Both sexes evolved reduction of ds3, but females lowered their mean more than the males. This resulted in a flip in dimorphism, from larger females to larger males, though both sexes evolved trait reduction. BUT DIMORPHISM SHRUNK THEN, AS THE DIFFERENCE BETWEEN MALES AND FEMALES IS NOW SMALLER??

time	cle	ds1	ds2	ds3	ect	lps	lpt	maf	mav	mcv	mdf	pmx	stl
1	0.913	0.215	0.359	0.203	0.865	0.428	0.853	0.944	0.391	0.507	0.959	0.948	0.883

time	cle	ds1	ds2	ds3	ect	lps	lpt	maf	mav	mcv	mdf	pmx	stl
2	0.942	0.212	0.325	0.180	0.891	0.404	0.853	0.948	0.520	0.520	0.963	0.967	0.908
3	0.843	0.207	0.249	0.153	0.770	0.279	0.803	0.965	0.289	0.525	0.977	0.912	0.777
4	0.890	0.210	0.249	0.201	0.830	0.372	0.741	0.977	0.435	0.589	0.986	0.935	0.831
5	0.954	0.211	0.211	0.195	0.909	0.377	0.756	0.985	0.533	0.622	0.992	0.975	0.921
6	0.885	0.211	0.134	0.171	0.820	0.291	0.686	0.991	0.645	0.456	0.996	0.949	0.811
7	0.812	0.211	0.124	0.239	0.760	0.340	0.617	0.994	0.224	0.717	0.999	0.879	0.747
8	0.928	0.210	0.135	0.258	0.885	0.387	0.706	0.994	0.342	0.730	1.000	0.969	0.872
9	0.899	0.213	0.145	0.304	0.857	0.406	0.715	0.995	0.521	0.756	1.000	0.940	0.845
10	0.954	0.217	0.235	0.555	0.940	0.571	0.810	0.997	0.454	0.719	1.000	0.976	0.935
11	0.913	0.211	0.162	0.476	0.875	0.388	0.703	0.997	0.363	0.657	1.000	0.957	0.864
12	0.949	0.221	0.262	0.726	0.929	0.585	0.803	0.997	0.462	0.595	1.000	0.968	0.926
13	0.904	0.220	0.260	0.789	0.885	0.598	0.795	0.998	0.470	0.370	1.000	0.929	0.872
14	0.925	0.220	0.280	0.883	0.906	0.659	0.854	0.997	0.526	0.472	1.000	0.958	0.898
15	0.880	0.225	0.283	0.839	0.849	0.617	0.796	0.997	0.490	0.398	1.000	0.919	0.834
16	0.953	0.216	0.276	0.931	0.931	0.614	0.831	0.997	0.414	0.541	1.000	0.975	0.925
17	0.803	0.219	0.232	0.832	0.765	0.383	0.655	0.996	0.569	0.758	1.000	0.854	0.751
18	0.780	0.212	0.225	0.817	0.726	0.297	0.558	0.995	0.705	0.722	0.999	0.859	0.717

time	cle	ds1	ds2	ds3	ect	lps	lpt	maf	mav	mcv	mdf	pmx	stl
1	0.500	0.500	0.500	0.500	0.500	0.500	0.500	0.500	0.500	0.500	0.500	0.500	0.500
2	0.514	0.504	0.509	0.495	0.512	0.508	0.517	0.495	0.396	0.490	0.495	0.511	0.513
3	0.636	0.514	0.559	0.516	0.628	0.601	0.602	0.475	0.523	0.480	0.476	0.626	0.641
4	0.563	0.509	0.544	0.459	0.558	0.539	0.672	0.456	0.436	0.450	0.458	0.556	0.562
5	0.543	0.507	0.551	0.417	0.539	0.522	0.687	0.436	0.389	0.425	0.439	0.537	0.544
6	0.618	0.512	0.589	0.415	0.613	0.579	0.716	0.415	0.317	0.522	0.419	0.612	0.620
7	0.591	0.510	0.601	0.364	0.589	0.564	0.712	0.379	0.546	0.382	0.383	0.588	0.592
8	0.539	0.507	0.579	0.324	0.536	0.514	0.683	0.373	0.478	0.368	0.378	0.537	0.540
9	0.524	0.506	0.586	0.299	0.521	0.510	0.636	0.355	0.408	0.340	0.359	0.523	0.522
10	0.379	0.497	0.544	0.203	0.377	0.400	0.578	0.321	0.438	0.359	0.324	0.385	0.373
11	0.531	0.508	0.605	0.226	0.528	0.517	0.685	0.301	0.528	0.403	0.303	0.530	0.533
12	0.363	0.492	0.547	0.150	0.360	0.386	0.566	0.284	0.439	0.436	0.284	0.369	0.358
13	0.373	0.495	0.555	0.133	0.372	0.386	0.561	0.269	0.432	0.575	0.268	0.378	0.371
14	0.326	0.496	0.548	0.102	0.326	0.349	0.514	0.255	0.399	0.514	0.253	0.334	0.323
15	0.365	0.492	0.552	0.107	0.365	0.373	0.502	0.250	0.433	0.554	0.247	0.368	0.367
16	0.361	0.497	0.574	0.084	0.360	0.381	0.570	0.234	0.462	0.463	0.229	0.369	0.356
17	0.561	0.504	0.629	0.116	0.559	0.542	0.669	0.226	0.364	0.313	0.219	0.559	0.565

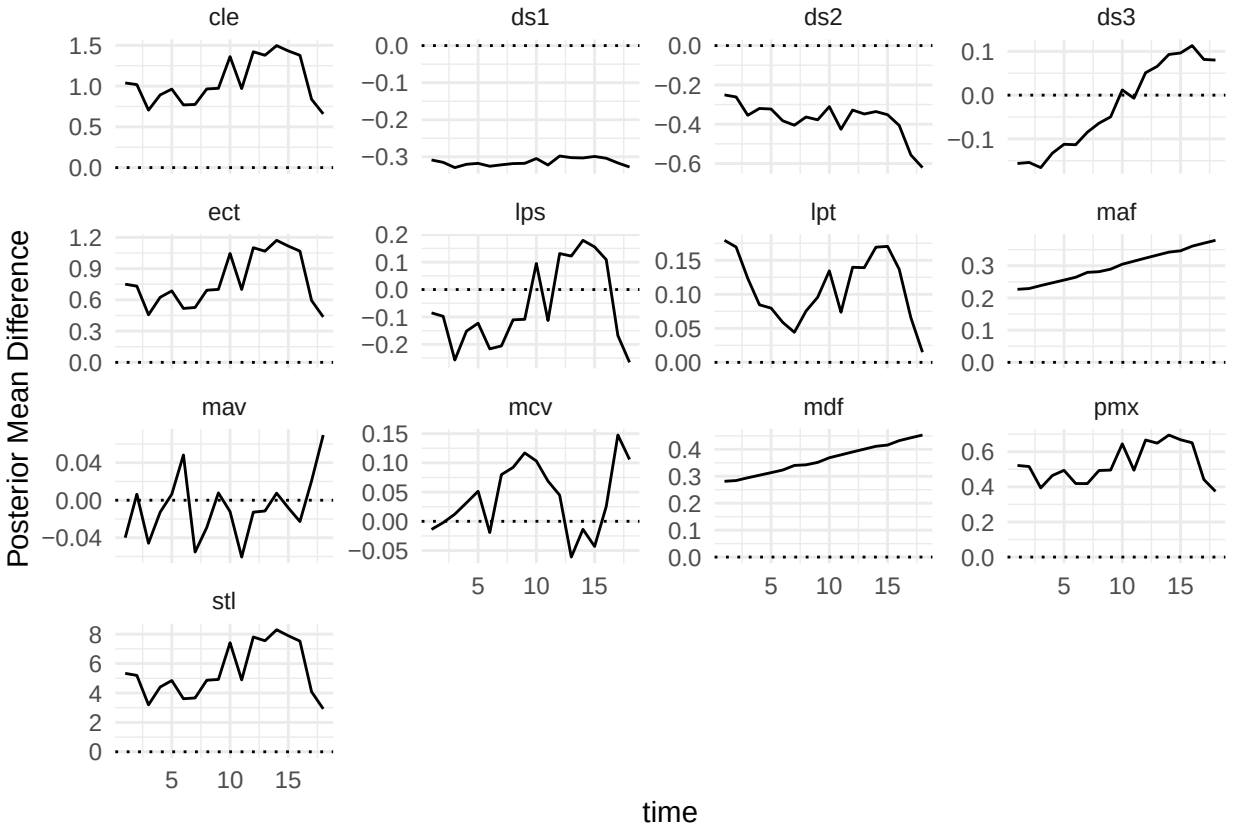

Figure 2: Posterior mean difference between males and females, in UNITS?. Values above 0 indicate larger male means

time	cle	ds1	ds2	ds3	ect	lps	lpt	maf	mav	mcv	mdf	pmx	stl
18	0.625	0.512	0.648	0.121	0.617	0.596	0.735	0.220	0.281	0.356	0.212	0.622	0.627

posterior mean difference for males versus females (values above 0 indicate means that were greater for males versus females)

5 Discussion, Future work and conclusions

We predicted that release from predators would result in niche expansion and increased sexual dimorphism, based on several studies of modern stickleback. For example, in lakes where sculpin competitors are absent and stickleback (Roesti et al. 2023) See Spoljaric and Reimchen 2008, page 512 right column for references and discussion of differences between benthic males and limnetic females. Male stickleback are benthic and littoral (Wootton 1976).... Reimchen papers in general good for this section. Moreover, tooth wear data

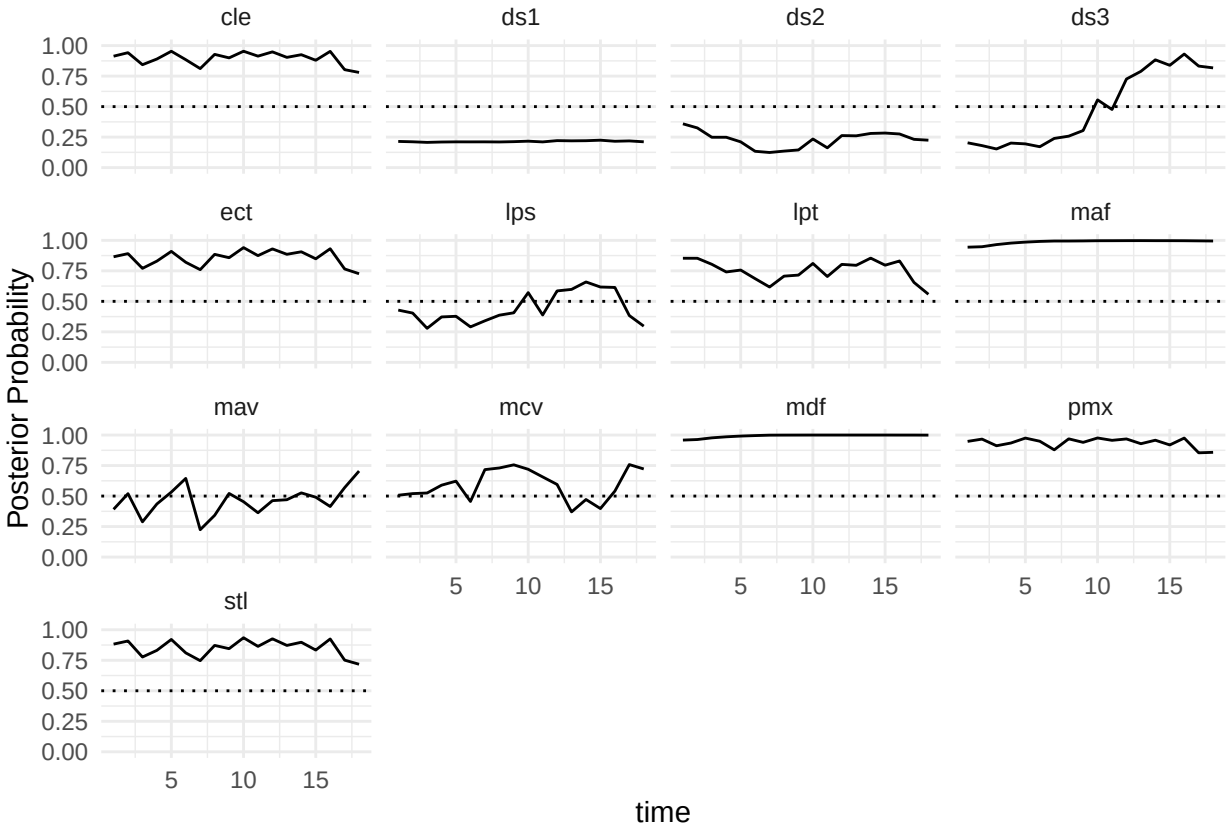

Figure 3: Posterior probabilities that the male posterior mean is larger than the female posterior mean

from the lineage II sequence suggest that individuals in this lineage began eating more planktonic prey over time, expanding toward an open-water niche from the benthic, bottom-feeding niche they started with (Purnell et al. 2007). That this expansion into open water by lineage II coincided with armor reduction is further indicative of a limnetic system with fewer salmonid piscivores (Schluter and McPhail (1992); Vamosi and Schluter (2004); Roesti et al. (2023)).

Acknowledgements

We thank O. Abughoush, S. Blain, A. Chaudhary, M. Islam, F. Joaquin, C. Lawson-Weinert, R. Sullivan, J. Tien, M.P. Travis, and W. Shim for help with data collection. We thank D. Schluter and S. Blain for loaning specimens and sharing data. We thank K. Swagel and C. McMahan of the Field Museum for assistance with specimen x-rays. This research was supported by NSF grants BSR-8111013, EAR-9870337, and DEB-0322818, the Center for Field Research (Earthwatch), and the National Geographic Society (2869-84) to MAB. It

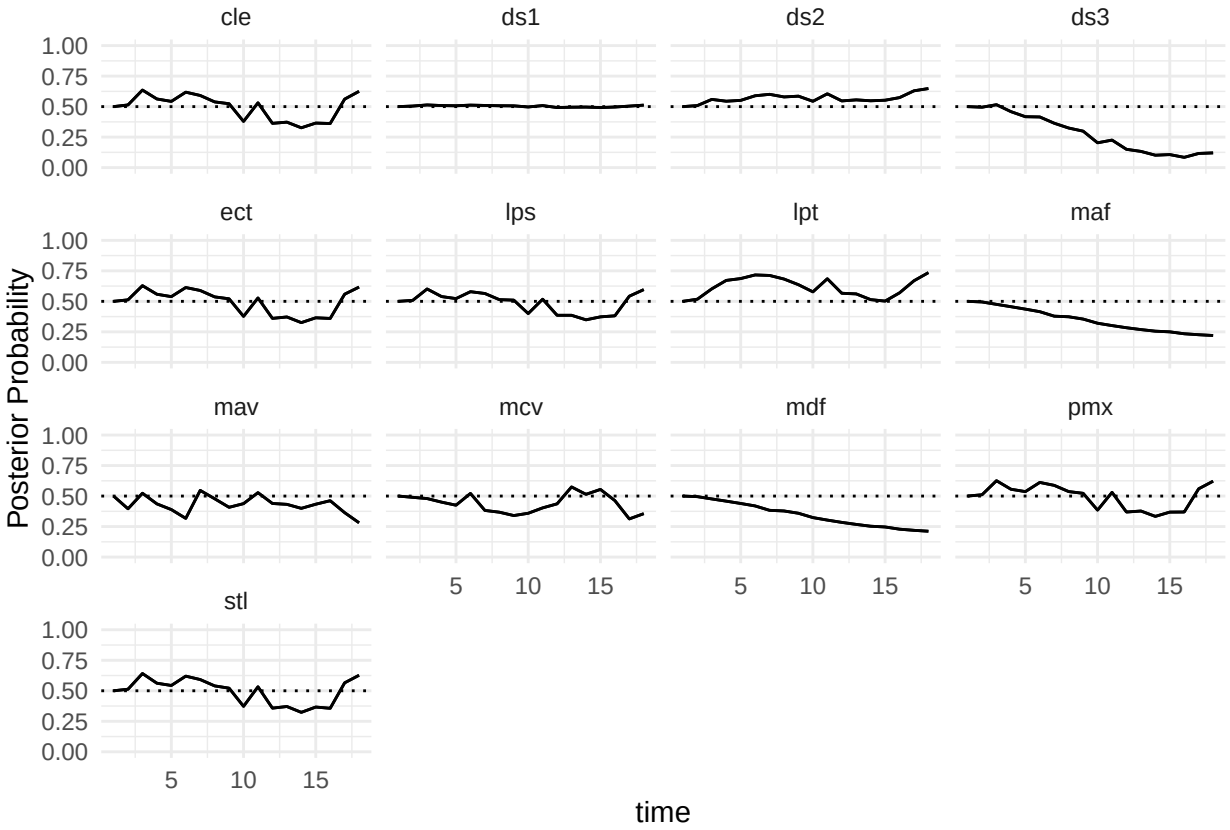

Figure 4: The Posterior Probability that male-female differences in subsequent samples are different from male-female differenceds in the initial sample. Values near 0.5 indicate little difference between the distributions. Values closer to 0 indicate that the difference in means has shifted towards larger means in females. Values closer to 1 indicate that the difference in means has shifted toward larger means in males.

was also supported by NSF grants DEB-1456462 and EAR-2145830 to YES. And NSF DMS-2015374 (GJM)

Supplementary Material

All code for reproducing the analyses in this paper is publicly available at https://github.com/Akhil-Ghosh/SticklebackProject

DIC results here.

5.1 Figures

References

Aguirre, W E, K Walker, and S Gideon. 2014. "Tinkering with the Axial Skeleton: Vertebral Number Variation in Ecologically Divergent Threespine Stickleback Populations." *Biological Journal of the Linnean Society* 113 (1): 204–19.

Baumgartner, J V, M A Bell, and P H Weinberg. 1988. "Body Form Differences Between the Enos Lake Species Pair of Threespine Sticklebacks (Gasterosteus Aculeatus Complex)." *Canadian Journal of Zoology* 66 (2): 467–74.

Bell, M A. 2009. "Implications of a Fossil Stickleback Assemblage for Darwinian Gradualism." *Journal of Fish Biology* 75 (8): 1977–99.

Bell, M A, J V Baumgartner, and E C Oslon. 1985. "Patterns of Temporal Change in Single Morphological Characters of a Miocene Stickleback Fish." *Paleobiology* 11: 258–71.

Bell, M A, G Orti, J A Walker, and J P Koenings. 1993. "Evolution of Pelvic Reduction in Threespine Sticklebacks: A Test of Competing Hypotheses." *Evolution* 47: 906–14.

Bell, M A, M P Travis, and D M Blouw. 2006. "Inferring Natural Selection in a Fossil Threespine Stickleback." *Paleobiology* 32 (4): 562–77.

Blain, S A. 2022. *Evolutionary Outcomes of Interactions Among Phenotypes in Post-Glacial Lakes*. University of British Columbia, Canada.

Bolnick, D I. 2011. "Sympatric Speciation in Threespine Stickleback: Why Not?" *International Journal of Ecology* 2011: 1–15.

Bolnick, D I, and M Doebeli. 2003. "Sexual Dimorphism and Adaptive Speciation: Two Sides of the Same Ecological Coin." *Evolution* 57 (11): 2433–49.

Bolnick, D I, and O L Lau. 2008. "Predictable Patterns of Disruptive Selection in Stickleback in Postglacial Lakes." *The American Naturalist* 172 (1): 1–11.

Bowne, P S. 1994. "Systematics and Morphology of the Gasterosteiformes." In *The Evolutionary Biology of the Threespine Stickleback*, edited by M A Bell and S A Foster. Oxford, UK: Oxford University Press.

Butler, Sawyer, M A, and J B Losos. 2007. "Sexual Dimorphism and Adaptive Radiation in Anolis Lizards." *Nature* 447 (7141): 202–5.

Buuren, Stef van, and Karin Groothuis-Oudshoorn. 2011. "Mice: Multivariate Imputation by Chained Equations in r." *Journal of Statistical Software* 45 (3): 1–67. https://doi.org/10.18637/jss.v045.i03.

Cerasoni, J N, M A Bell, and Y E Stuart. 2024. "Geology, Microstratigraphy, and Paleontology of Truckee Formation Lacustrine Diatomite Deposits Near Hazen, Nevada, USA, with Emphasis on Fossil Stickleback Fish." *PaleoBios* 41: 1–15.

Cooper, I A, R T Gilman, and J W Boughman. 2011. "Sexual Dimorphism and Speciation on Two Ecological Coins: Patterns from Nature and Theoretical Predictions." *Evolution*

65 (9): 2553–71.

Cornuault, J. 2022. "Bayesian Analyses of Comparative Data with the Ornstein–Uhlenbeck Model: Potential Pitfalls." *Systematic Biology* 71 (6): 1524–40. https://doi.org/10.1093/sysbio/syac036.

De Lisle, S P, S Paiva, and L Rowe. 2018. "Habitat Partitioning During Character Displacement Between the Sexes." *Biology Letters* 14: 20180124.

De Lisle, S P, and L Rowe. 2015. "Ecological Character Displacement Between the Sexes." *The American Naturalist* 186: 693–707.

———. 2017. "Disruptive Natural Selection Predicts Divergence Between the Sexes During Adaptive Radiation." *Ecology and Evolution* 7: 3590–3601.

Godfrey, L R, S K Lyon, and M R Sutherland. 1993. "Sexual Dimorphism in Large-Bodied Primates: The Case of the Subfossil Lemurs." *American Journal of Physical Anthropology* 90: 315–34.

Hendry, A P, D I Bolnick, D Berner, and C L Peichel. 2009. "Along the Speciation Continuum in Sticklebacks." *Journal of Fish Biology* 75 (8): 2000–2036.

Herrmann, N C, J T Stroud, and J B Losos. 2021. "The Evolution of 'Ecological Release' into the 21st Century." *Trends in Ecology and Evolution* 36 (3): 206–15.

Hone, D W E, and J C Mallon. 2017. "Protracted Growth Impedes the Detection of Sexual Dimorphism in Non-Avian Dinosaurs." *Palaeontology* 60 (4): 535–45.

Hunt, G, M A Bell, and M P Travis. 2008. "Evolution Toward a New Adaptive Optimum: Phenotypic Evolution in a Fossil Stickleback Lineage." *Evolution* 62 (3): 700–710.

Koscinski, K, and S Pietraszewski. 2004. "Methods to Estimate Sexual Dimorphism from Unsexed Samples: A Test with Computer Generated Samples." *Przeglad Antropologiczny - Anthropological Review* 67: 33–55.

Little, R. J. A., and D. B. Rubin. 2002. *Statistical Analysis with Missing Data*. Wiley Series in Probability and Mathematical Statistics. Probability and Mathematical Statistics. Wiley. http://books.google.com/books?id=aYPwAAAAMAAJ.

Mallon, J C. 2017. "Recognizing Sexual Dimorphism in the Fossil Record: Lessons from Nonavian Dinosaurs." *Paleobiology* 43 (3): 495–507.

Parent, C E, and B J Crespi. 2009. "Ecological Opportunity in Adaptive Radiation of Galapagos Endemic Land Snails." *The American Naturalist* 174: 898–905.

Pfennig, D W, and K S Pfennig. 2012. *Evolution's Wedge: Competition and the Origins of Diversity*. University of California Press, Berkeley, USA.

Reimchen, T E. 1994. "Predators and Morphological Evolution in Threespine Stickleback." In *The Evolutionary Biology of the Threespine Stickleback*, edited by M A Bell and S A Foster. Oxford, UK: Oxford University Press.

Reimchen, T E, and P Nosil. 2004. "Variable Predation Regimes Predict the Evolution of Sexual Dimorphism in a Population of Threespine Stickleback." *Evolution* 58 (6): 1274–81.

Roesti, M, J S Groh, S A Blain, M Huss, P Rassias, D I Bolnick, Y E Stuart, C L Peichel, and D Schluter. 2023. "Species Divergence Under Competition and Shared Predation." *Ecology Letters* 26: 111–23.

Saitta, T, M T Stockdale, N R Longrich, V Bonhomme, M J Benton, I C Cuthill, and P J Makovicky. 2020. "An Effect Size Statistical Framework for Investigating Sexual Dimorphism in Non-Avian Dinosaurs and Other Extinct Taxa." *Biological Journal of the Linnean Society* 131 (2): 231–73. https://doi.org/10.1093/biolinnean/blaa105.

Schindelin, J, I Arganda-Carreras, E Frise, V Kaynig, M Longair, T Pietzsch, S Preibisch, C Rueden, S Saalfeld, and B Schmid. 2012. "Fiji: An Open-Source Platform for Biological-Image Analysis." *Nature Methods* 9: 976–682.

Schluter, D, and J D McPhail. 1992. "Ecological Character Displacement and Speciation in Sticklebacks." *The American Naturalist* 140 (1): 85–108.

Schoener, T W. 1968. "The Anolis Lizards of Bimini: Resource Partitioning in a Complex Fauna." *Ecology* 29: 704–26.

Shine, R. 1989. "Ecological Causes for the Evolution of Sexual Dimorphism: A Review of the Evidence." *The Quarterly Review of Biology* 64 (4): 419–61.

Siddiqui, R, S Swank, A Ozark, F Joaquin, M P Travis, C D McMahan, M A Bell, and Y E Stuart. 2024. "Inferring the Evolution of Reproductive Isolation in a Lineage of Fossil Threespine Stickleback, Gasterosteus Doryssus." *Proceedings of the Royal Society B* 291: 20240337.

Stuart, Y E, J W Sherwin, A Kamath, and T Veen. 2021. "Male and Female Anolis Carolinensis Maintain Their Dimorphism Despite the Presence of Novel Interspecific Competition." *Evolution* 75 (11): 2708–16.

Stuart, Y E, M P Travis, and M A Bell. 2020. "Inferred Genetic Architecture Underlying Evolution in a Fossil Stickleback Lineage." *Nature Ecology and Evolution* 4 (11): 1549–57.

Stuart, Y E, T Veen, J N Weber, D Hanson, M Ravinet, B K Lohman, C J Thompson, et al. 2017. "Contrasting Effects of Environment and Genetics Generate a Continuum of Parallel Evolution." *Nature Ecology and Evolution* 1 (6): 158.

Team, R Core. 2022. *R: A Language and Environment for Statistical Computing*. Vienna, Austria: R Foundation for Statistical Computing. https://www.R-project.org/.

Uhlenbeck, G E, and L S Ornstein. 1930. "On the Theory of the Brownian Motion." *Phys. Rev.* 36 (September): 823–41. https://doi.org/10.1103/PhysRev.36.823.

Vamosi, S M, and D Schluter. 2004. "Character Shifts in the Defensive Armor of Sympatric Sticklebacks." *Evolution* 58: 376–85.

Voje, K L, M A Bell, and Y E Stuart. 2022. "Evolution of Static Allometry and Constraint on Evolutionary Allometry in a Fossil Stickleback." *Journal of Evolutionary Biology* 35 (3): 423–38.

Zhou, X, and J Reiter. 2010. "A Note on Bayesian Inference After Multiple Imputation." *The American Statistician* 64 (2): 159–63.

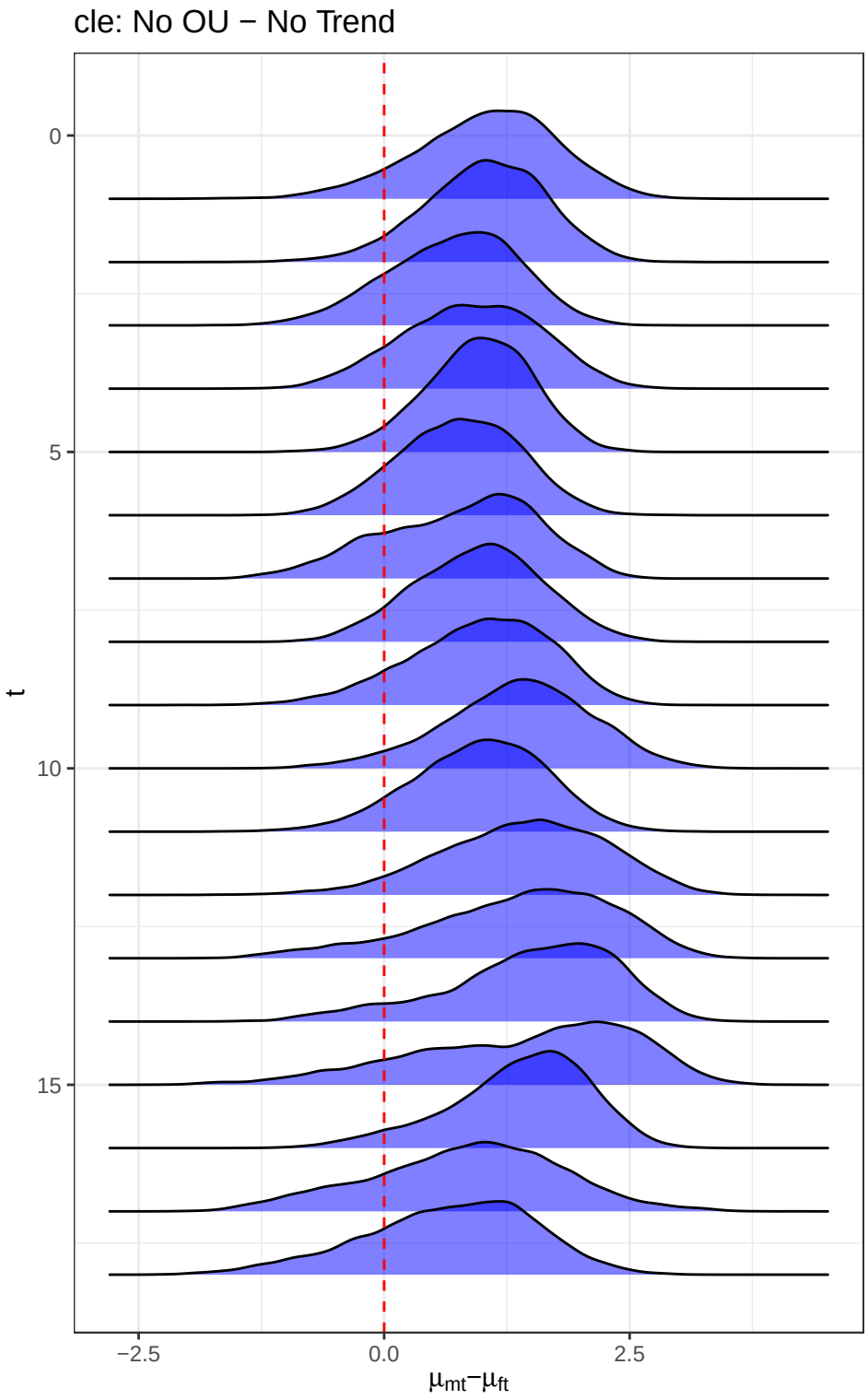

Figure 5: cle

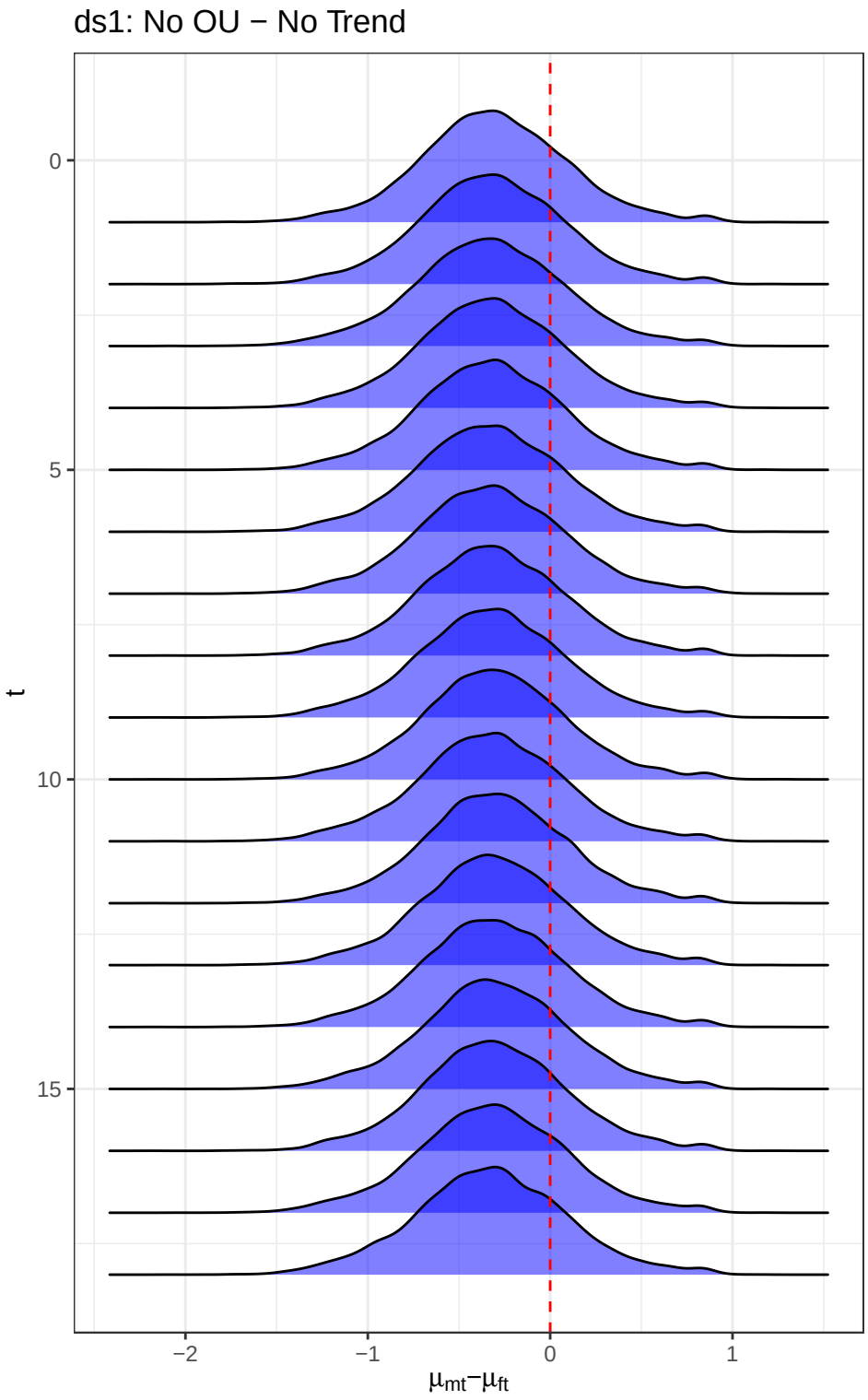

Figure 6: ds1

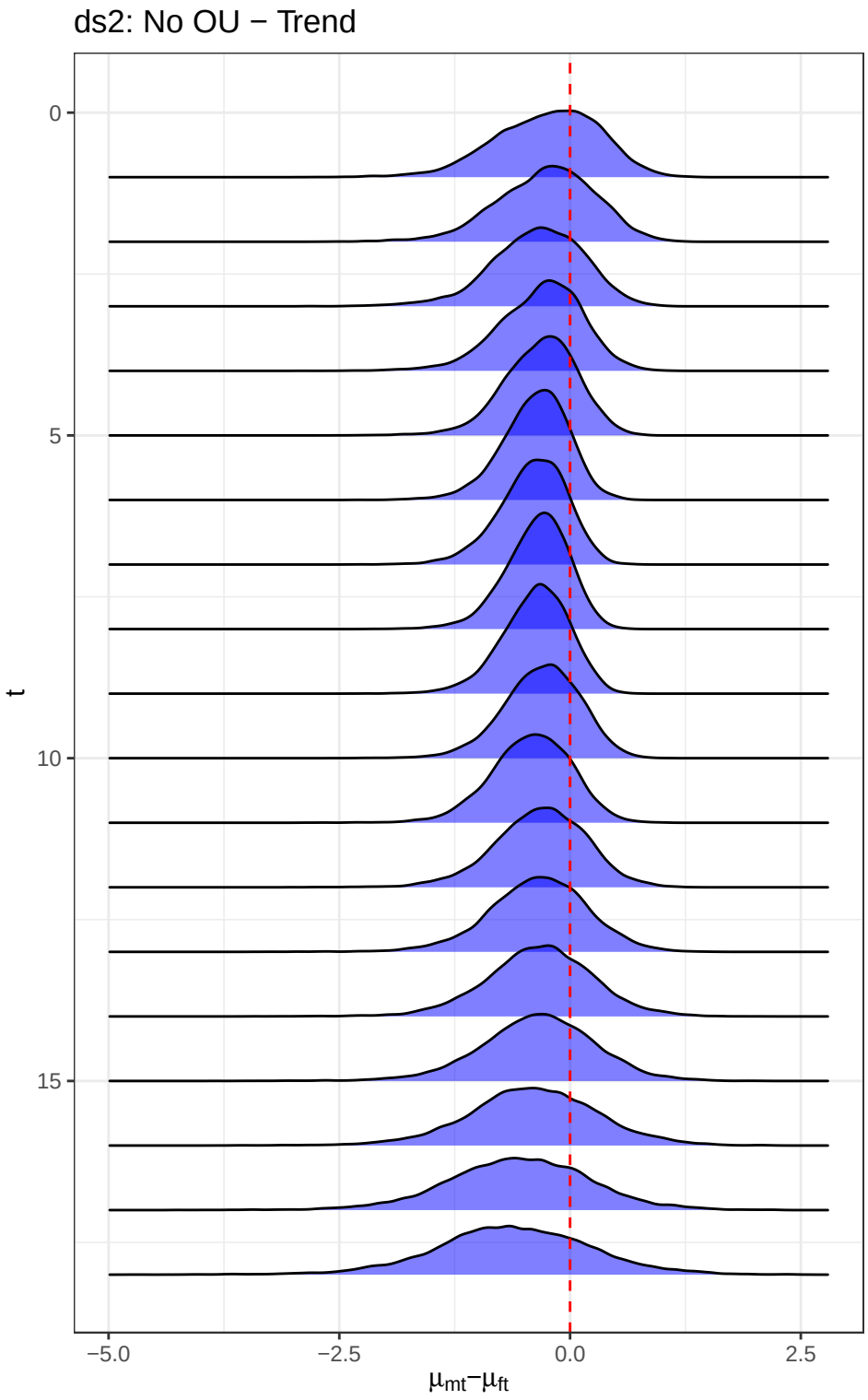

Figure 7: ds2

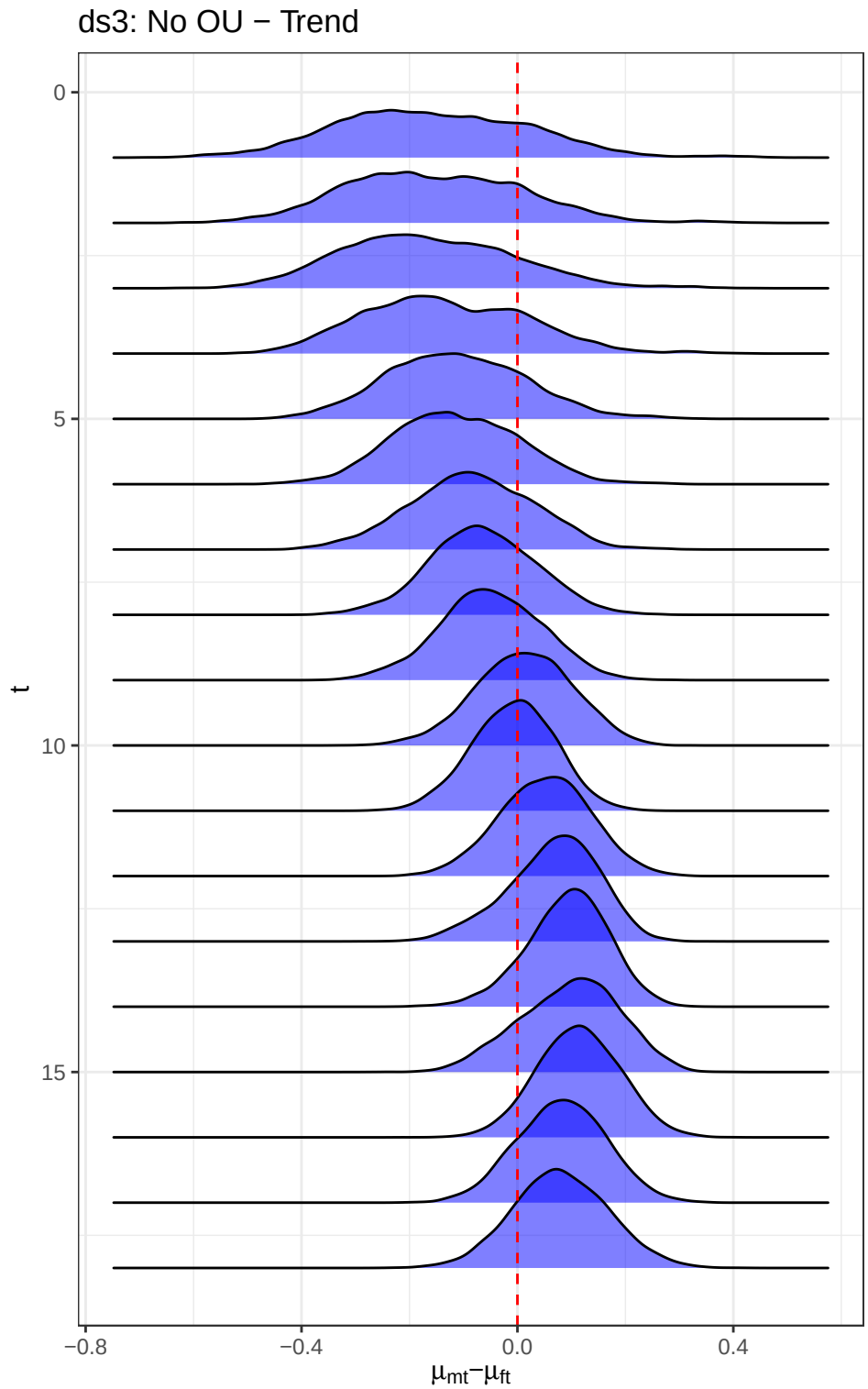

Figure 8: ds3

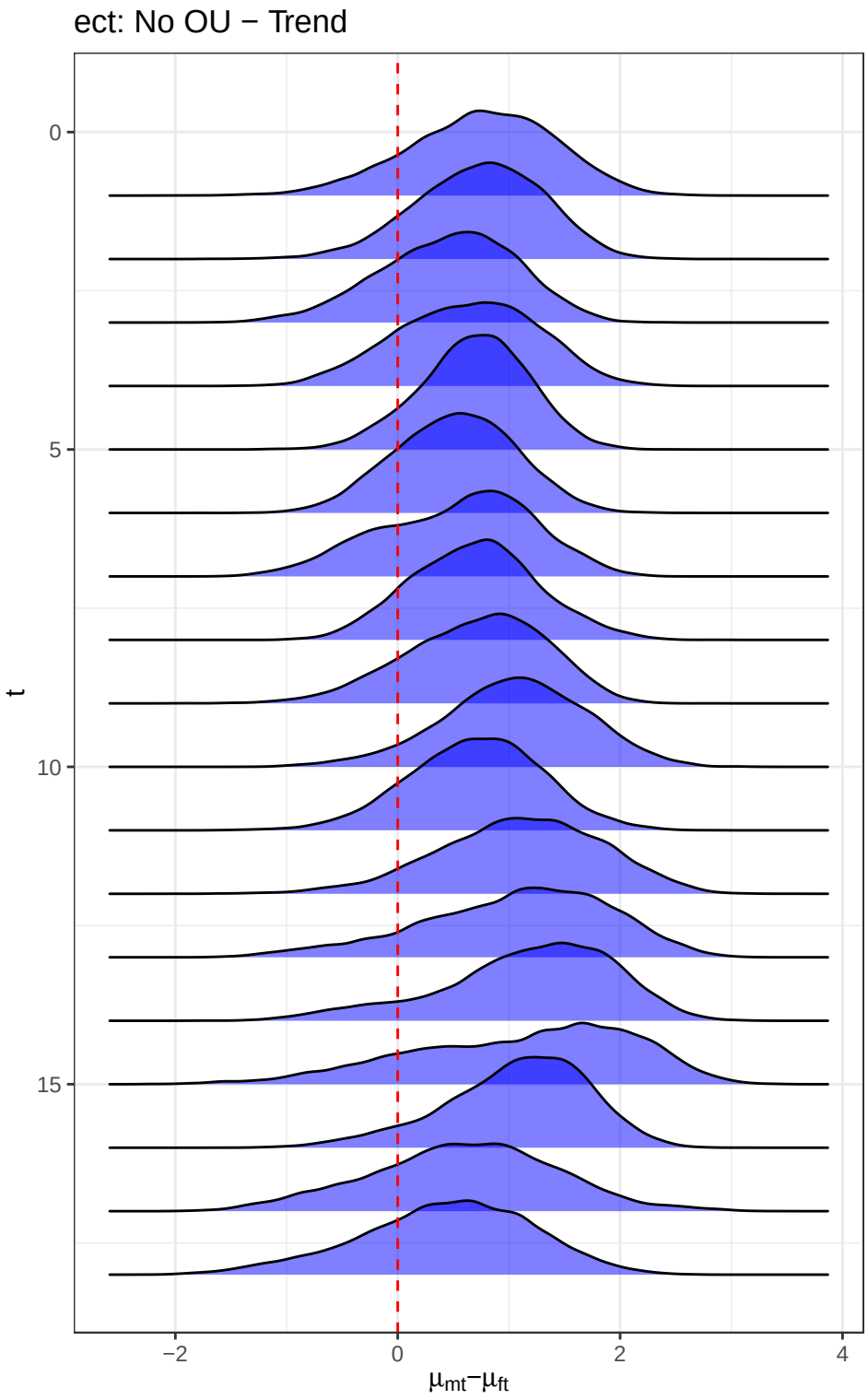

Figure 9: ect

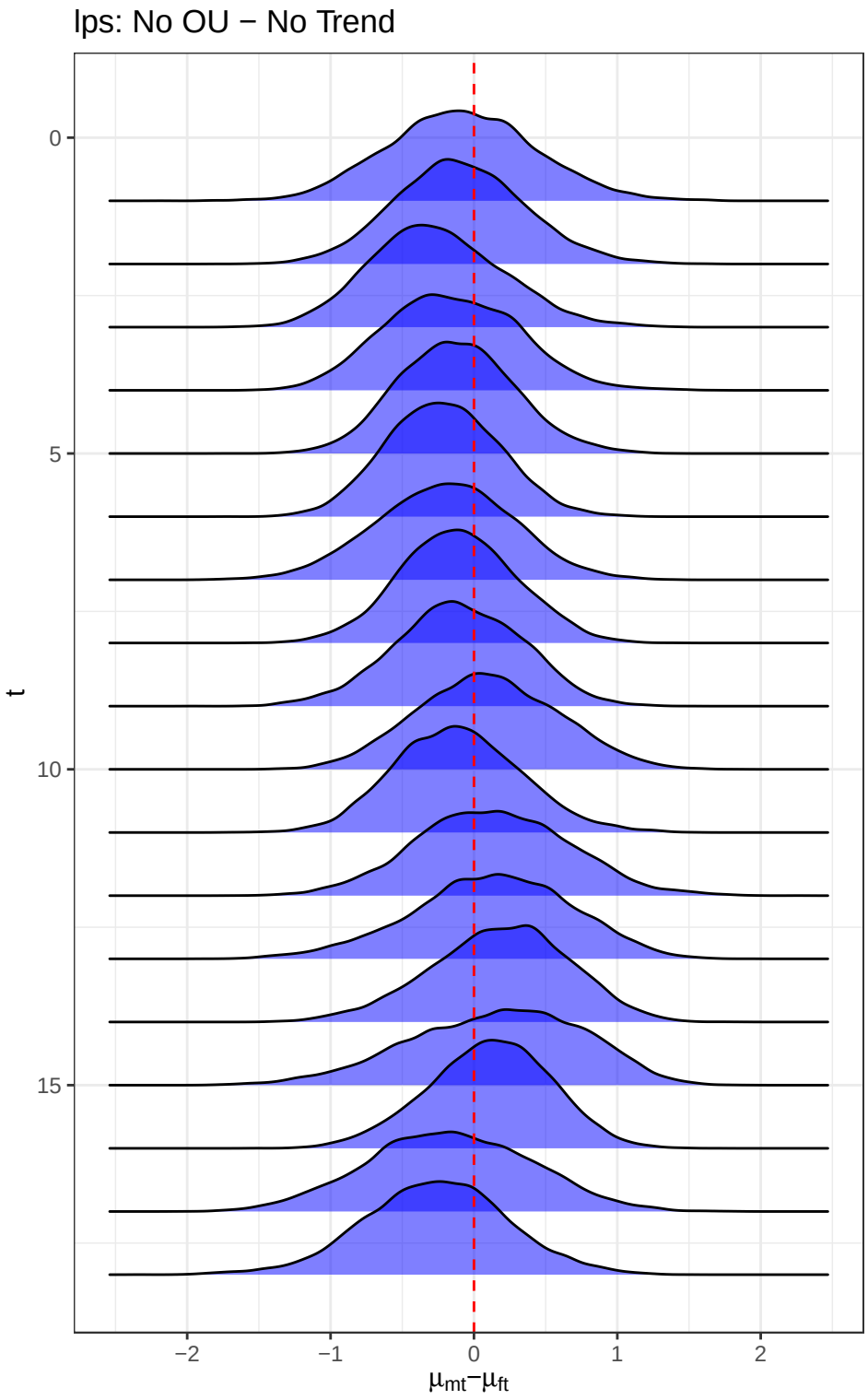

Figure 10: lps

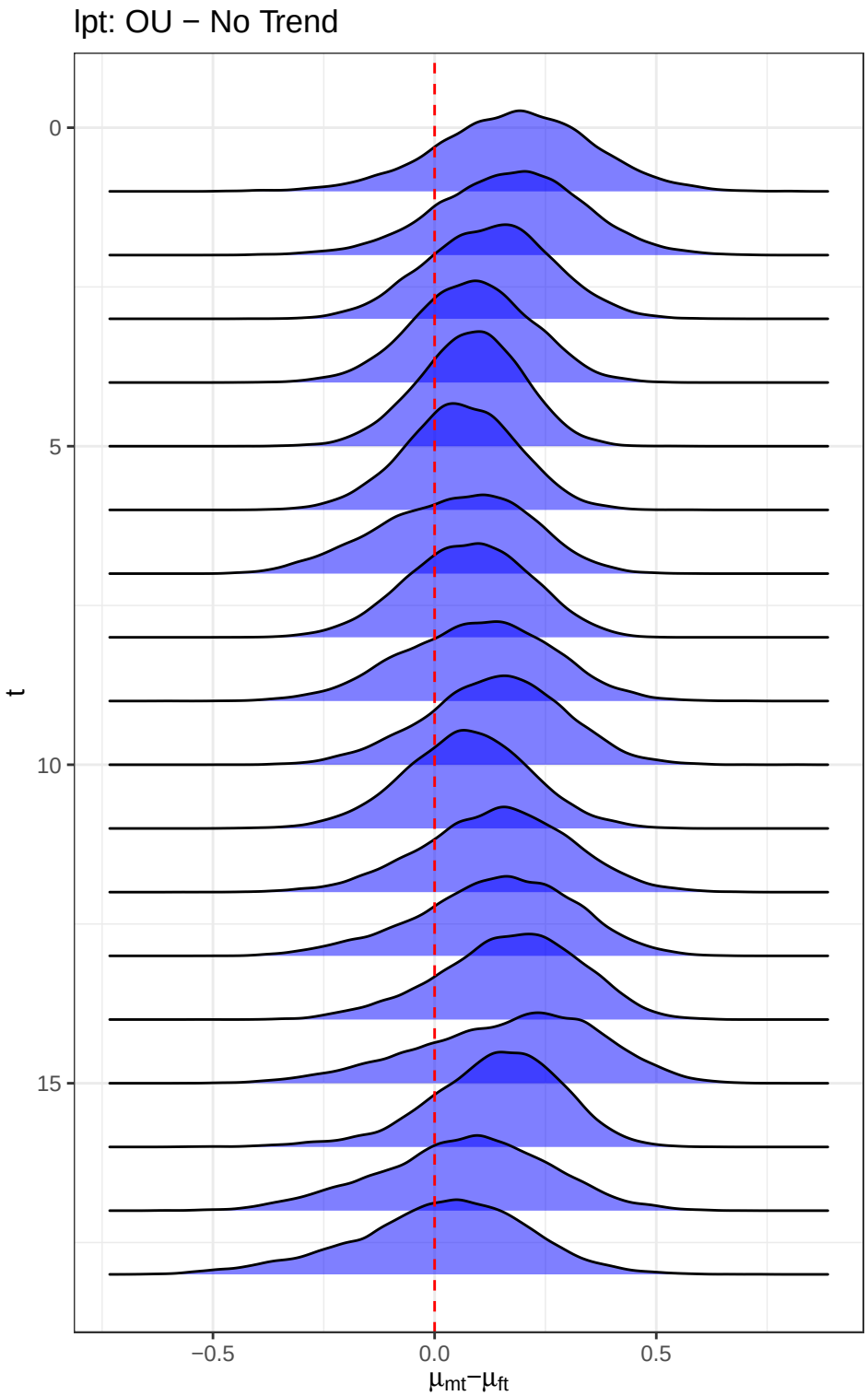

Figure 11: lpt

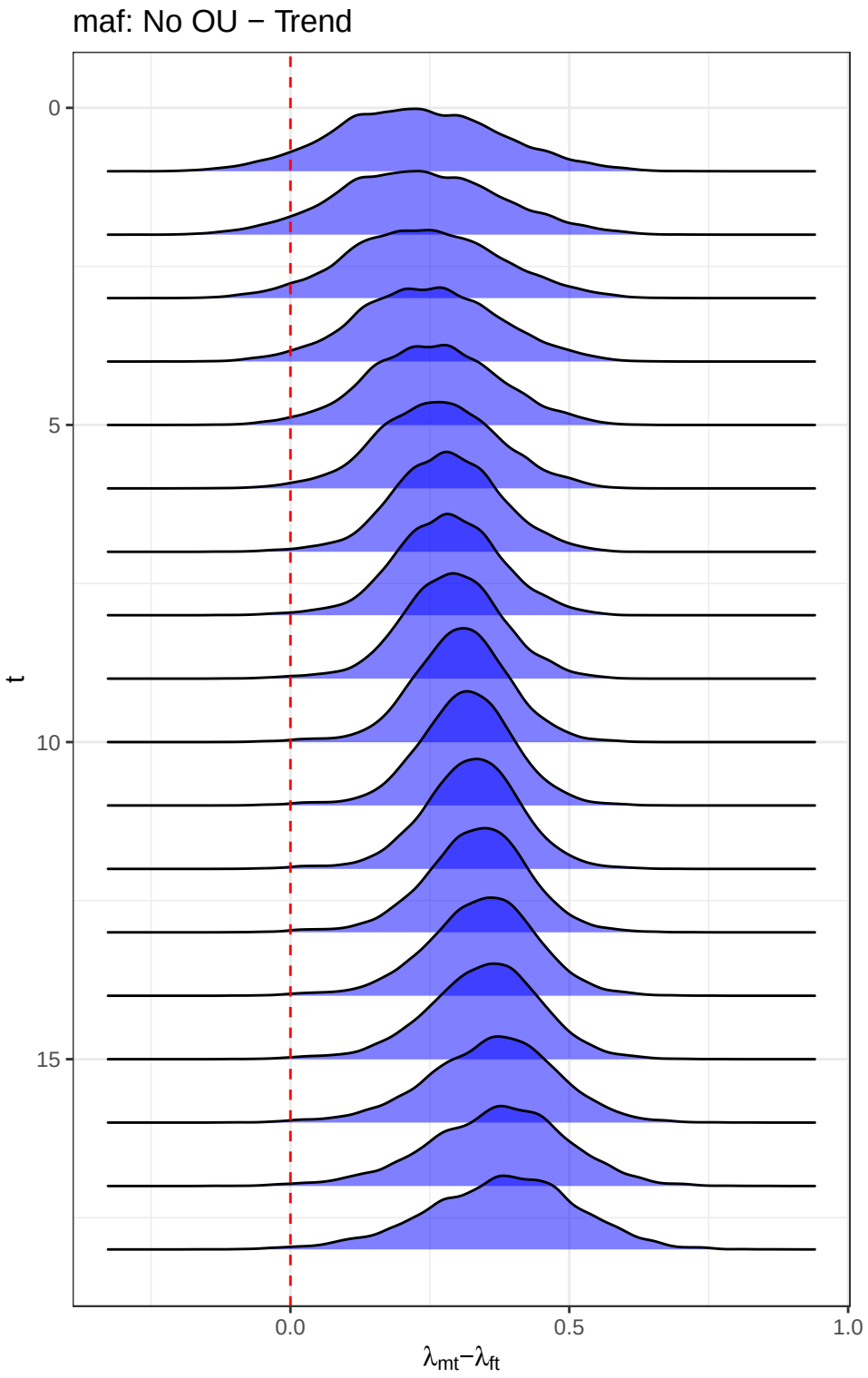

Figure 12: maf

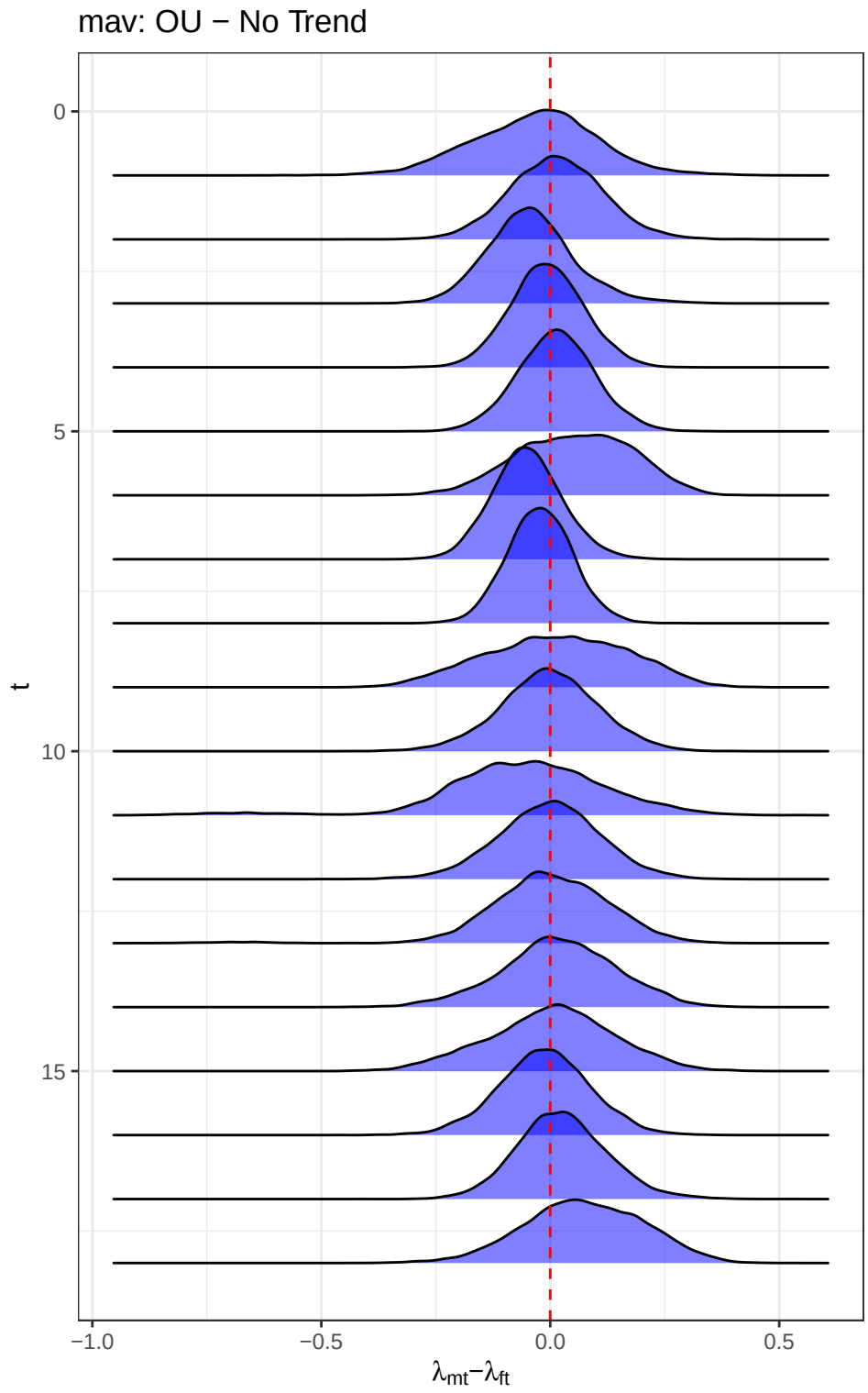

Figure 13: mav

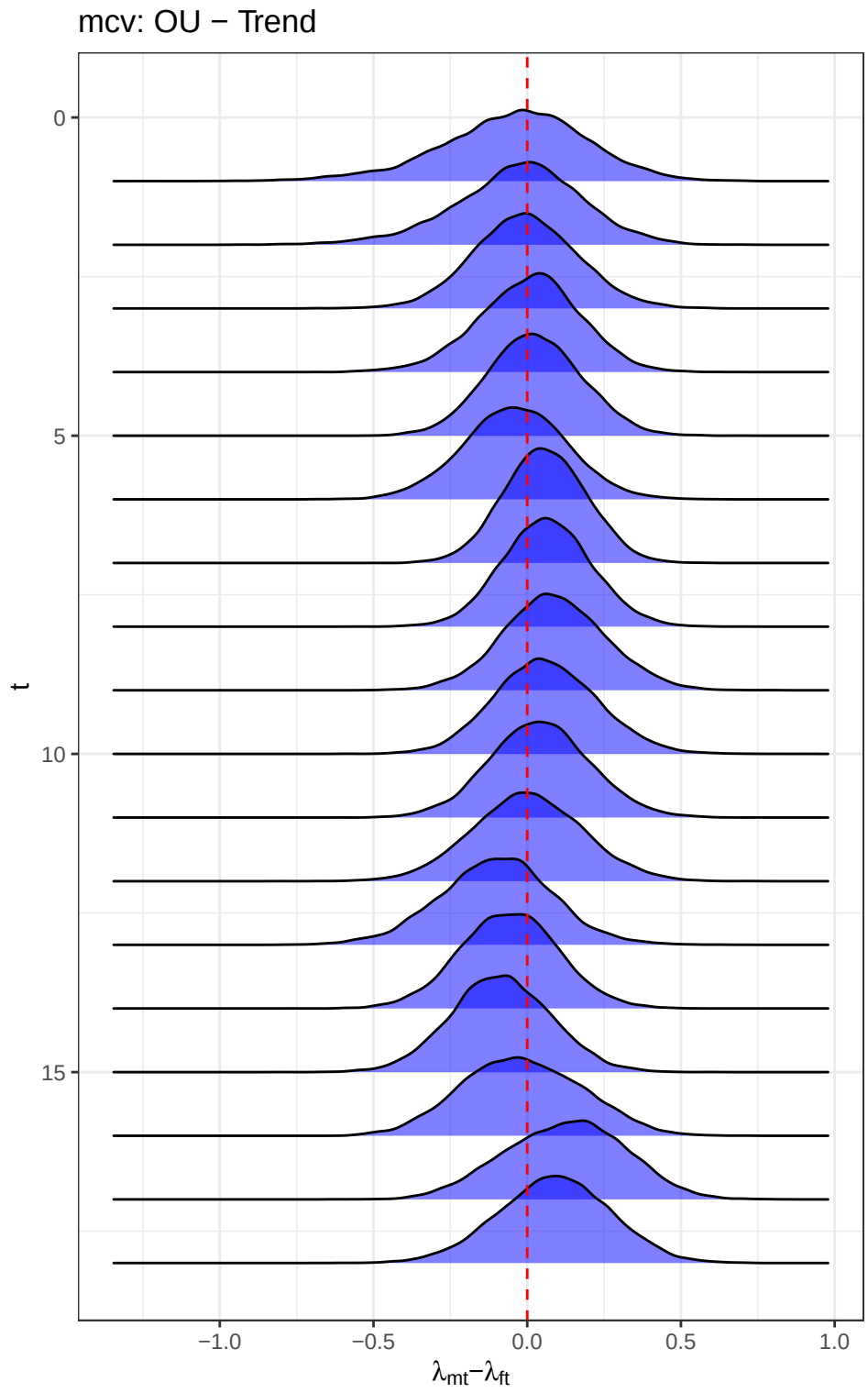

Figure 14: mcv

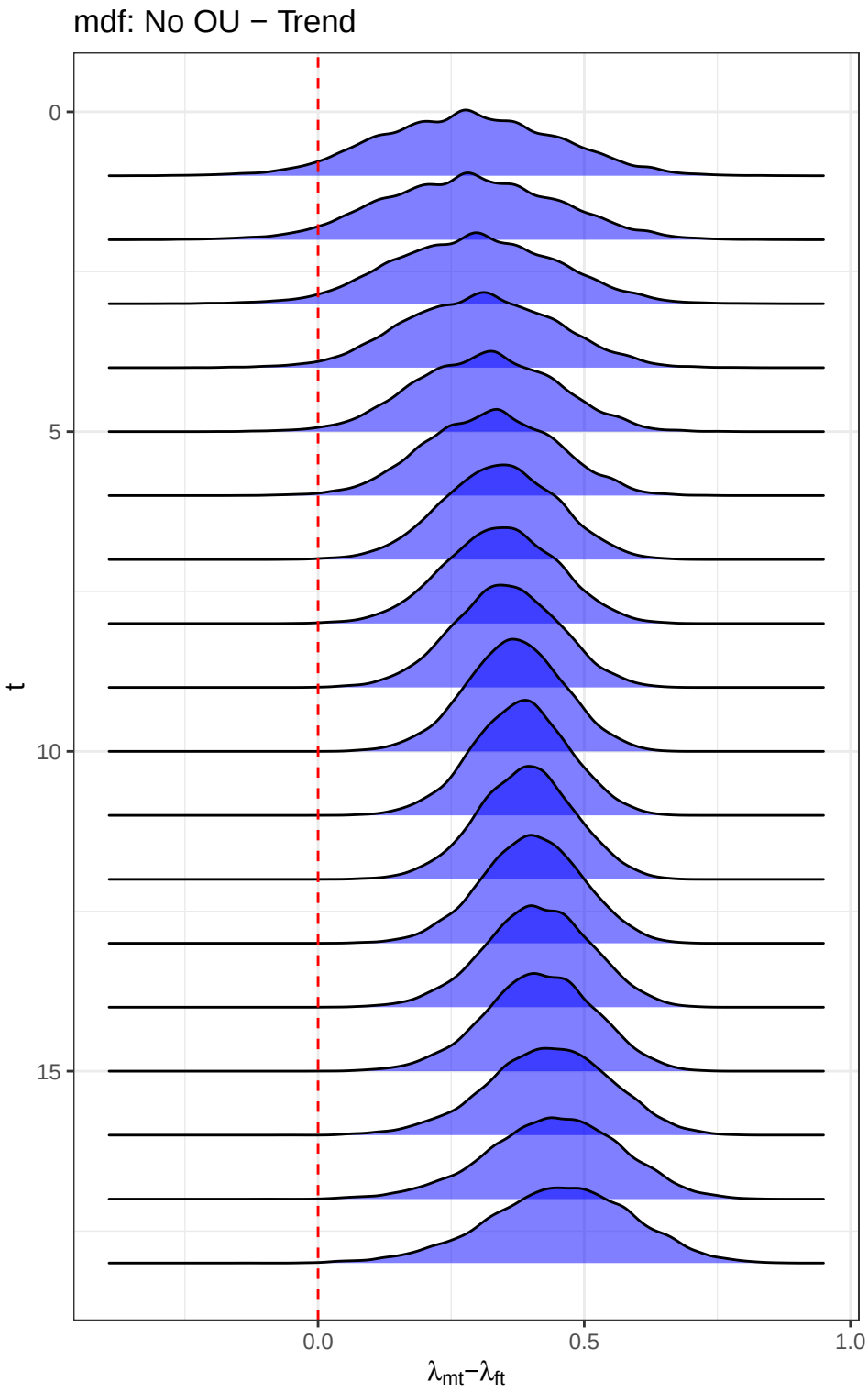

Figure 15: mdf

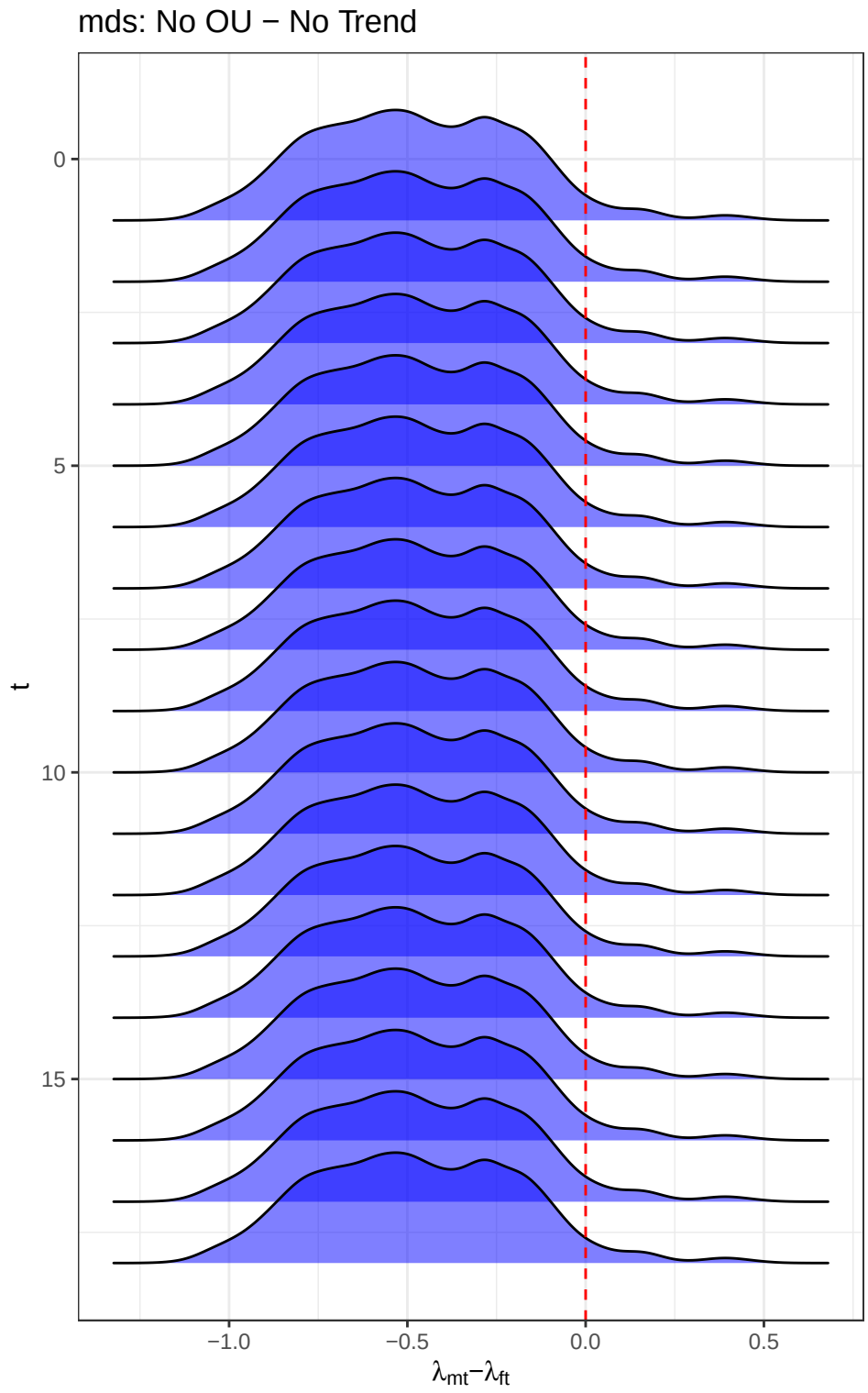

Figure 16: mds

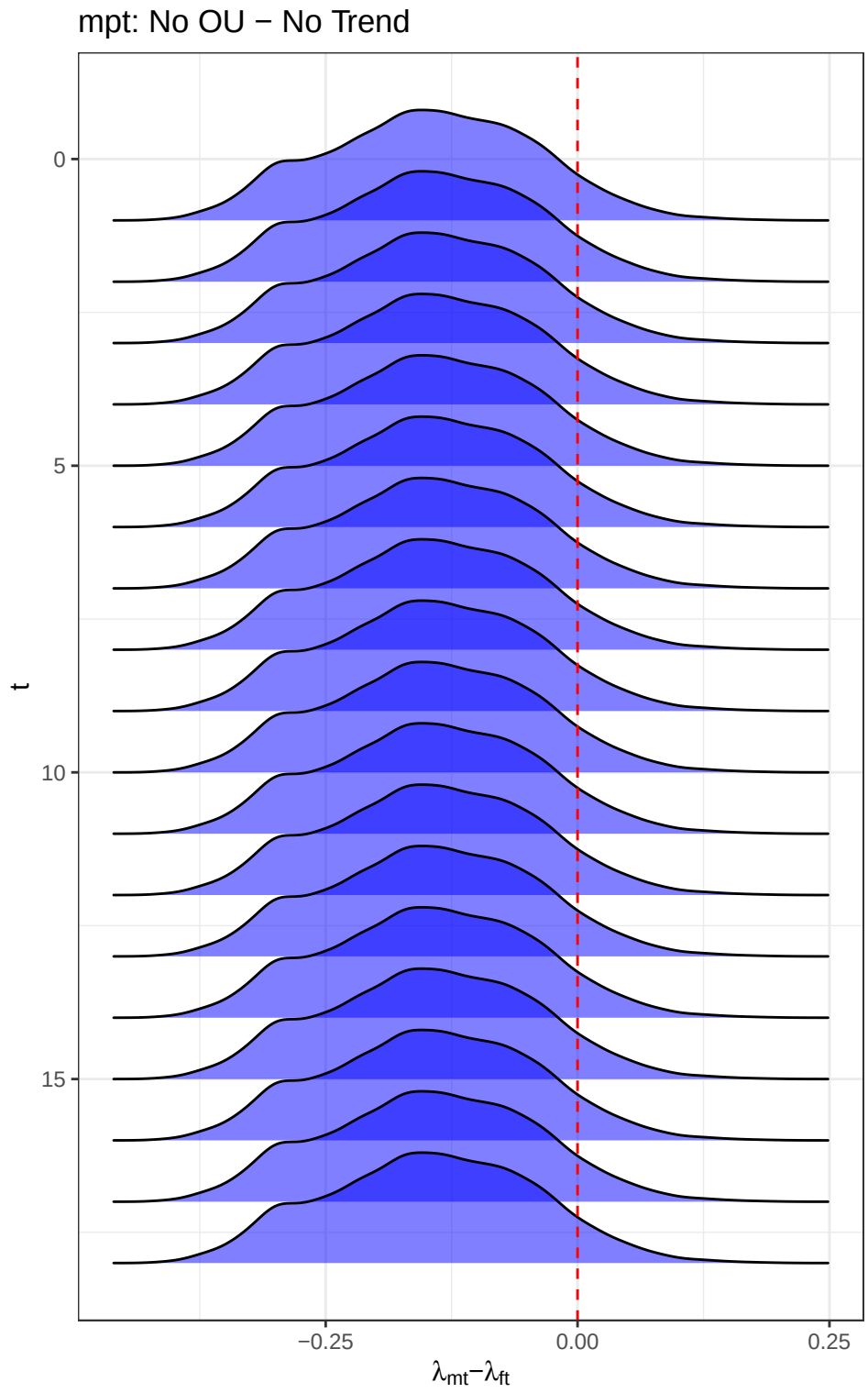

Figure 17: mpt

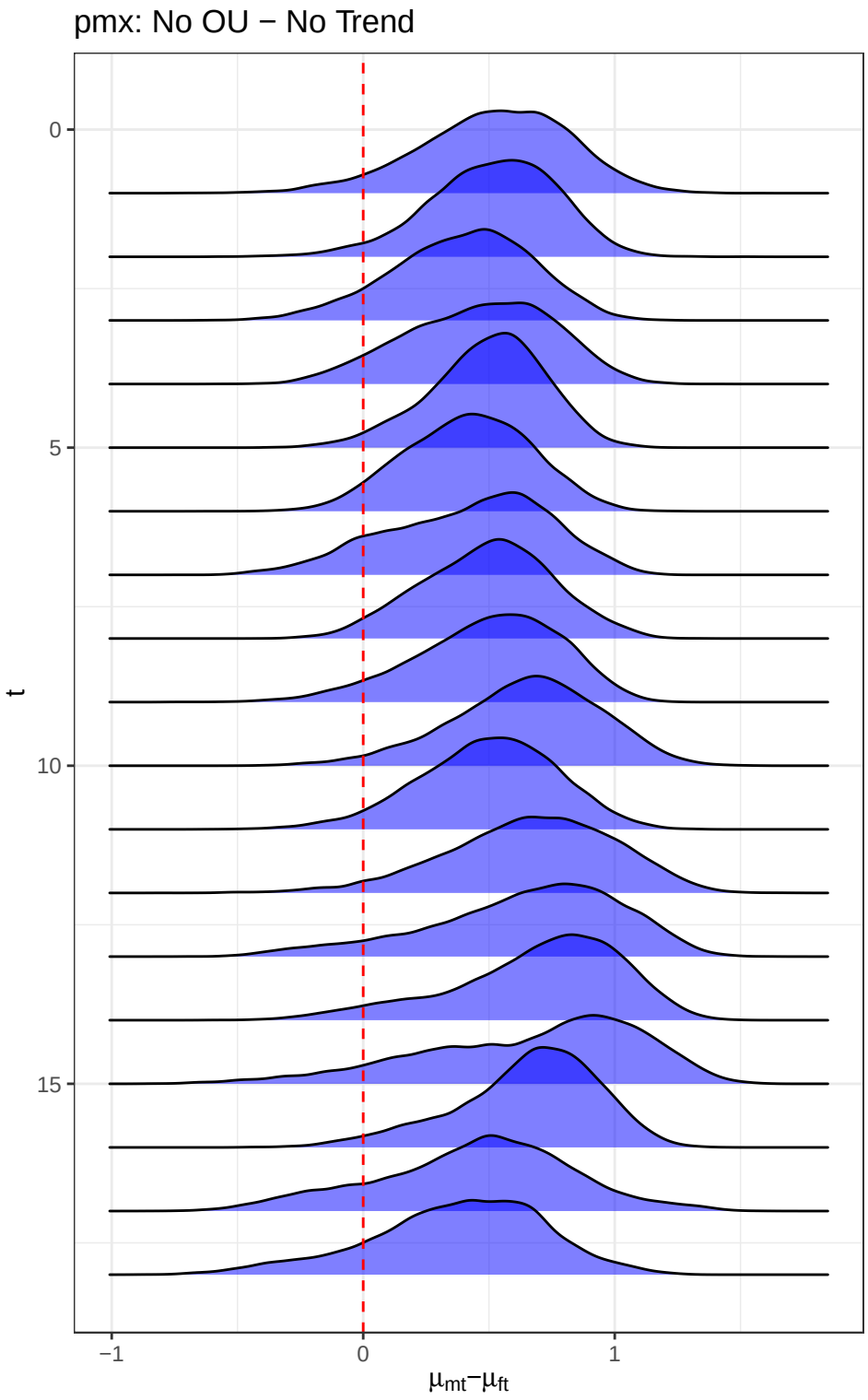

Figure 18: pmx

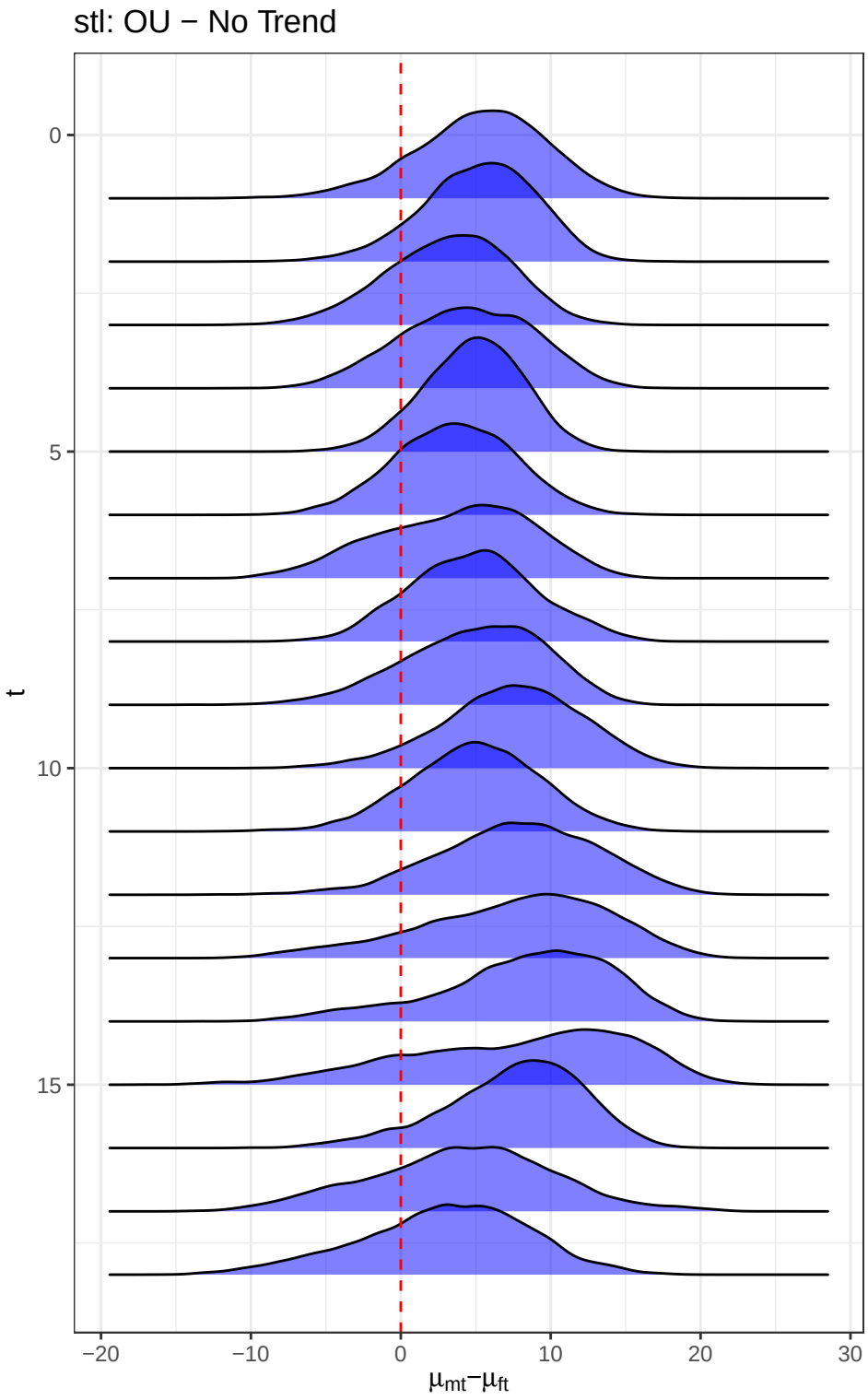

Figure 19: stl